Supporting Information

Mechanochemical Synthesis of Crystalline U(VI) Triperoxide Solids

Dmytro V. Kravchuk and Dr. Tori Z. Forbes*

Department of Chemistry, University of Iowa, Iowa City, Iowa 52242, United States

* Correspondence to: tori-forbes@uiowa.edu

Table of Contents

Powder X-ray Diffraction

Raman Spectroscopy

Infrared Spectroscopy

Scanning Electron Microscopy

Powder X-ray Diffraction

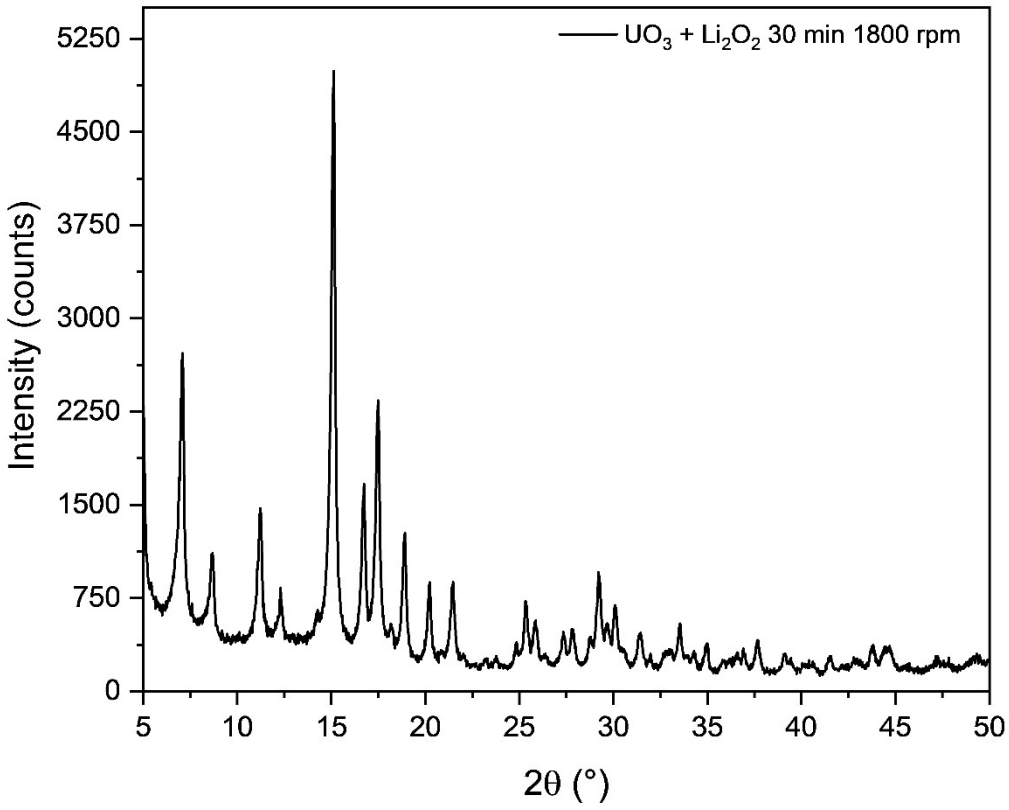

Figure S1: Raw PXRD pattern of m_{30}-UO_3-Li_2O_2

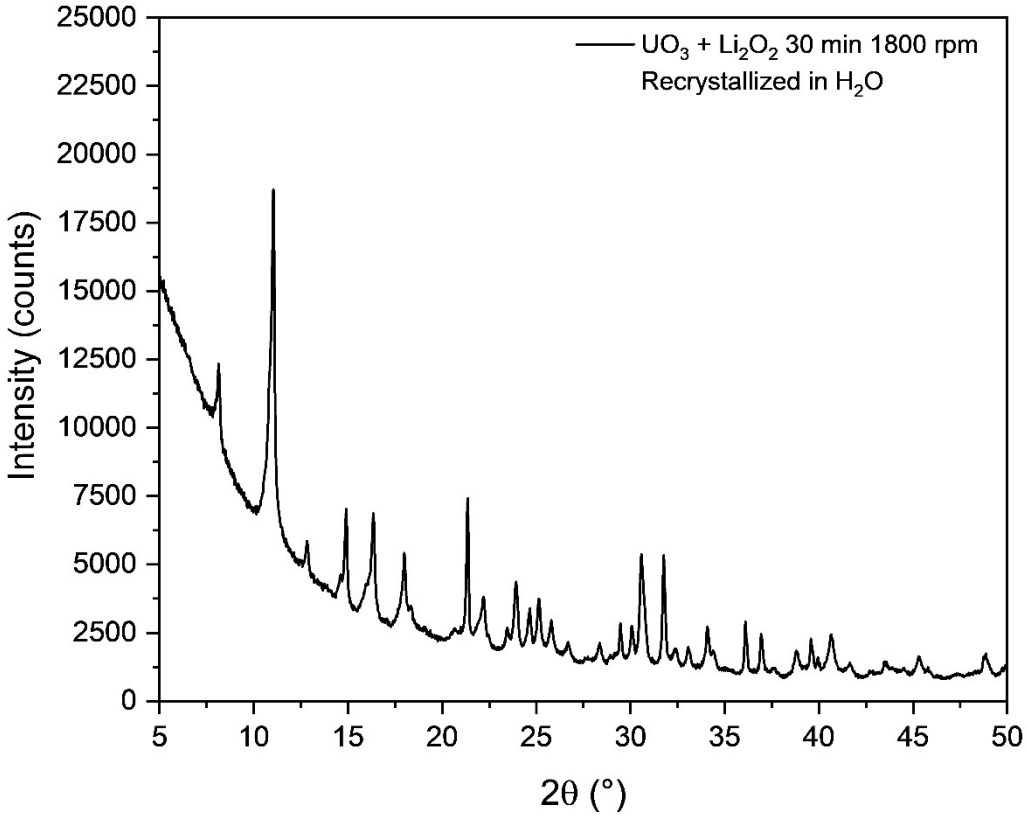

Figure S2: Raw PXRD pattern of recrystallized m_{30}-UO_3-Li_2O_2

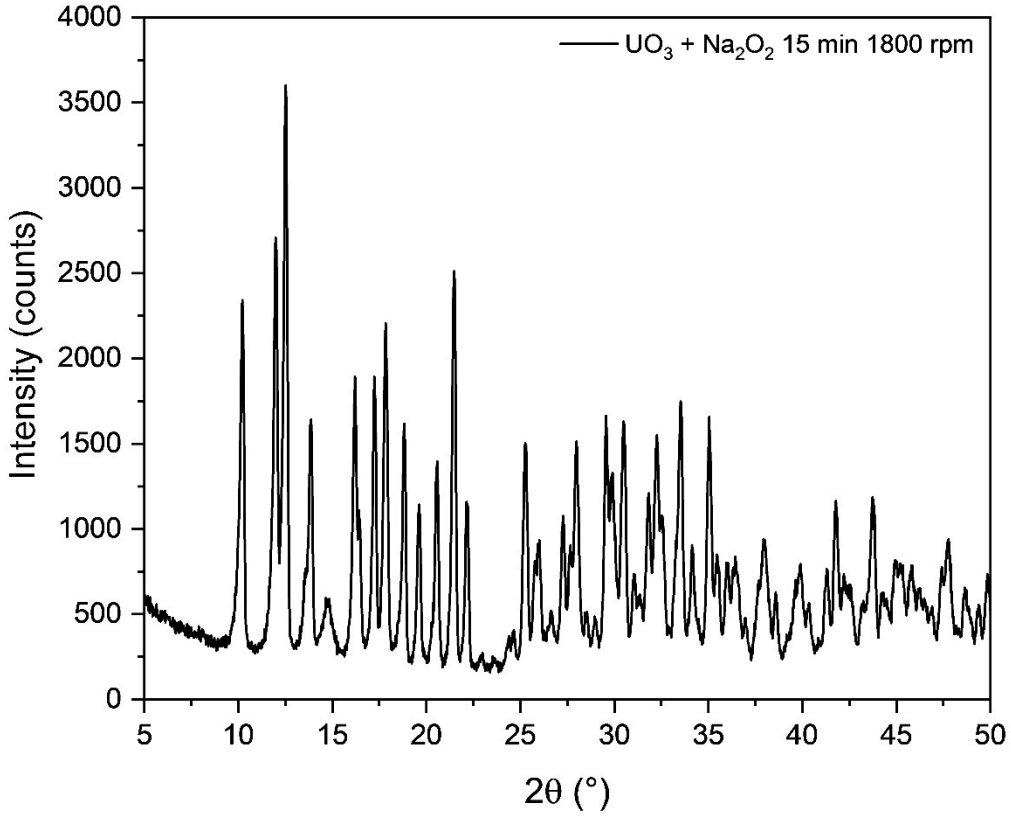

Figure S3: Raw PXRD pattern of m_{15}-UO_3-Na_2O_2

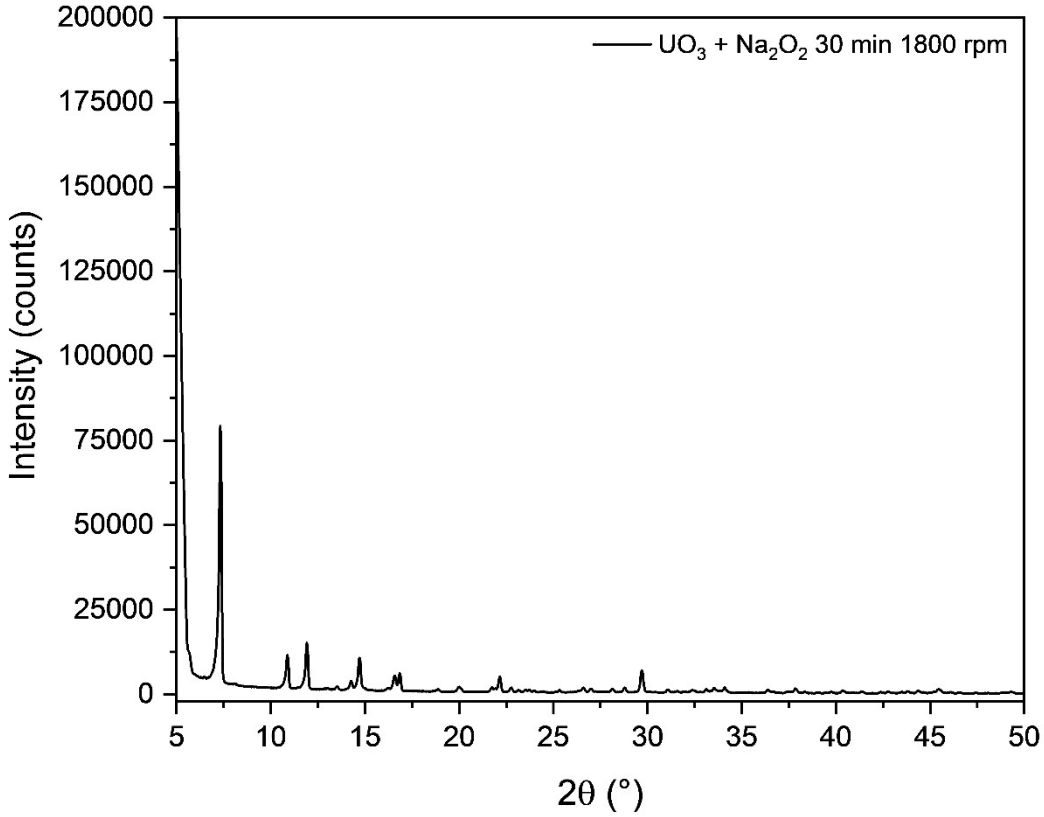

Figure S4: Raw PXRD pattern of m_{30}-UO_3-Na_2O_2

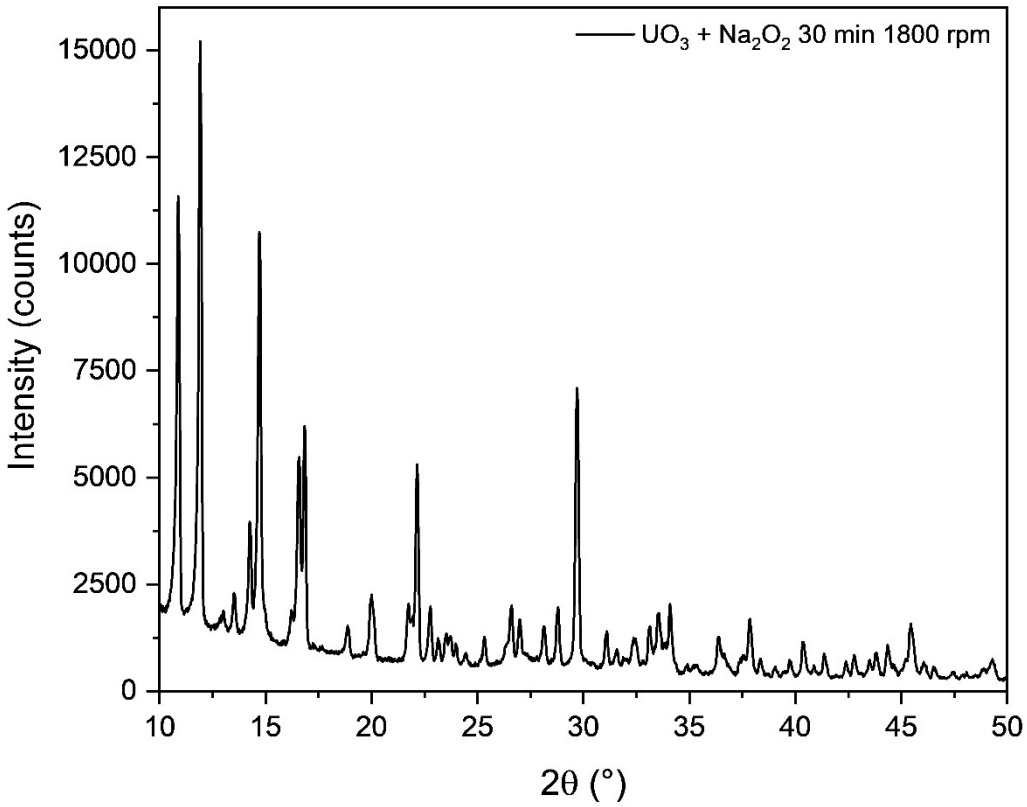

Figure S5: Raw PXRD pattern of m_{30}-UO_3-Na_2O_2 enhanced 2θ 10°-50°

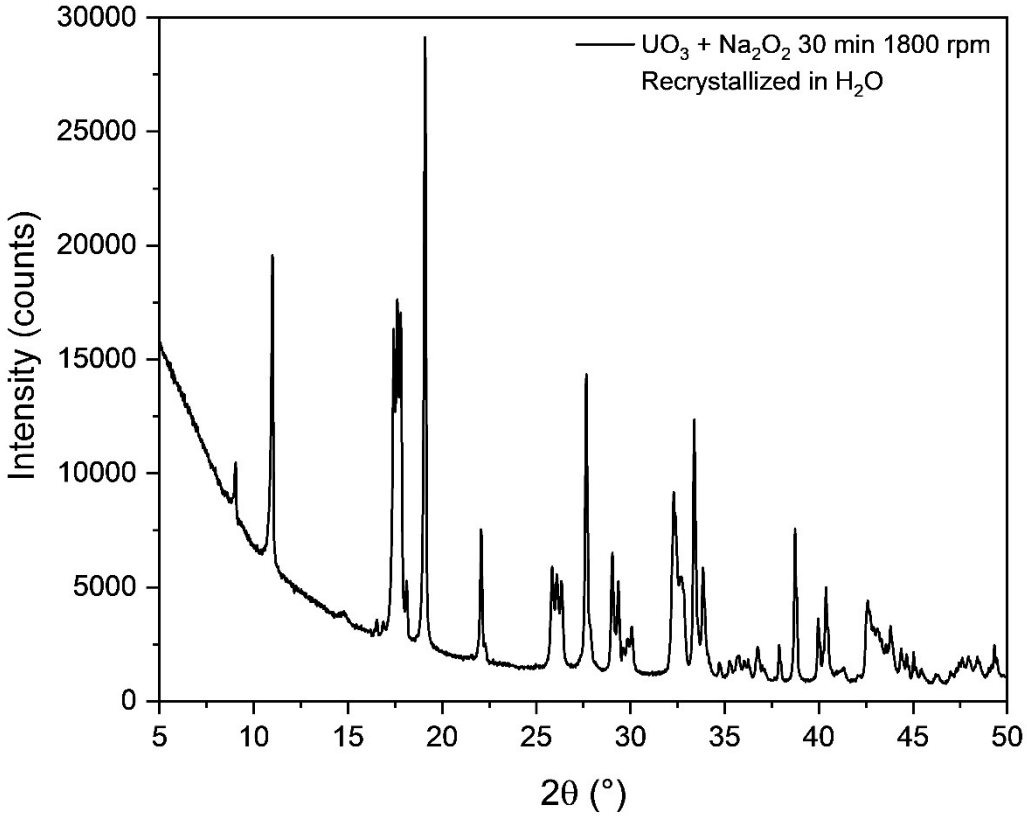

Figure S6: Raw PXRD pattern of recrystallized m_{30}-UO_3-Na_2O_2

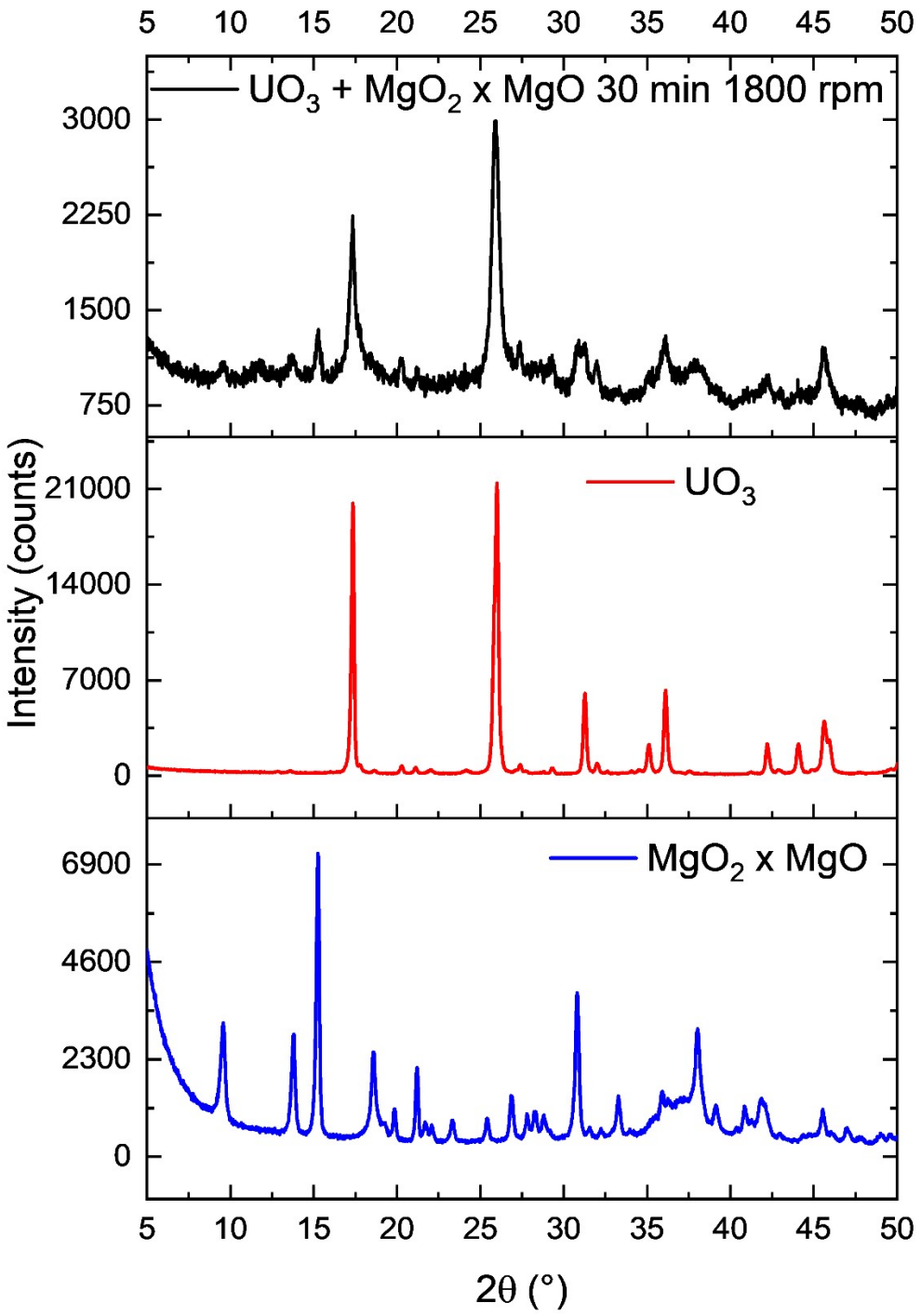

Figure S7: Raw PXRD patterns of UO_3 + MgO_2 30 min 1800 rpm and starting materials

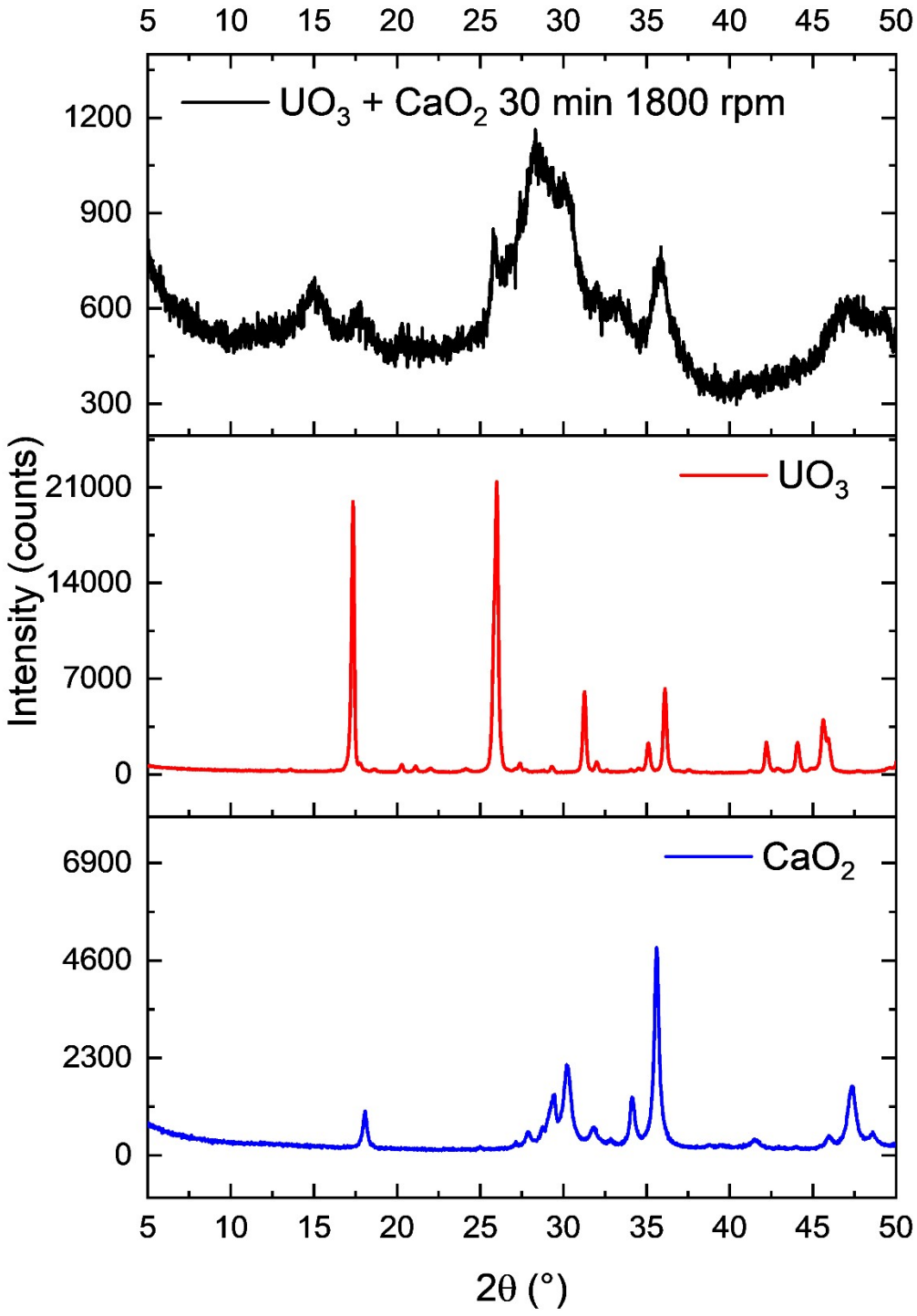

Figure S8: Raw PXRD patterns of UO_3 + CaO_2 30 min 1800 rpm and starting materials

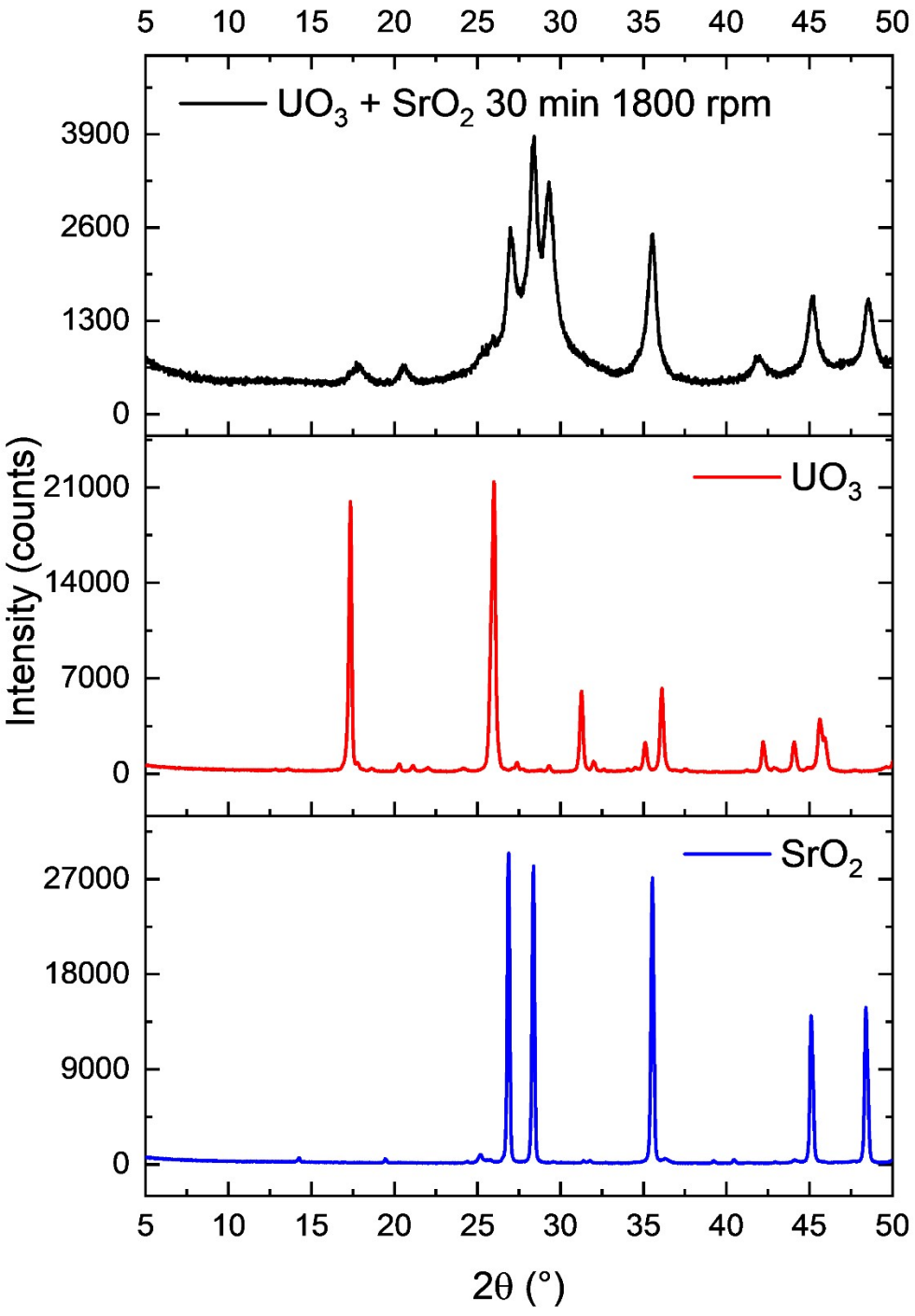

Figure S9: Raw PXRD patterns of UO_3 + SrO_2 30 min 1800 rpm and starting materials

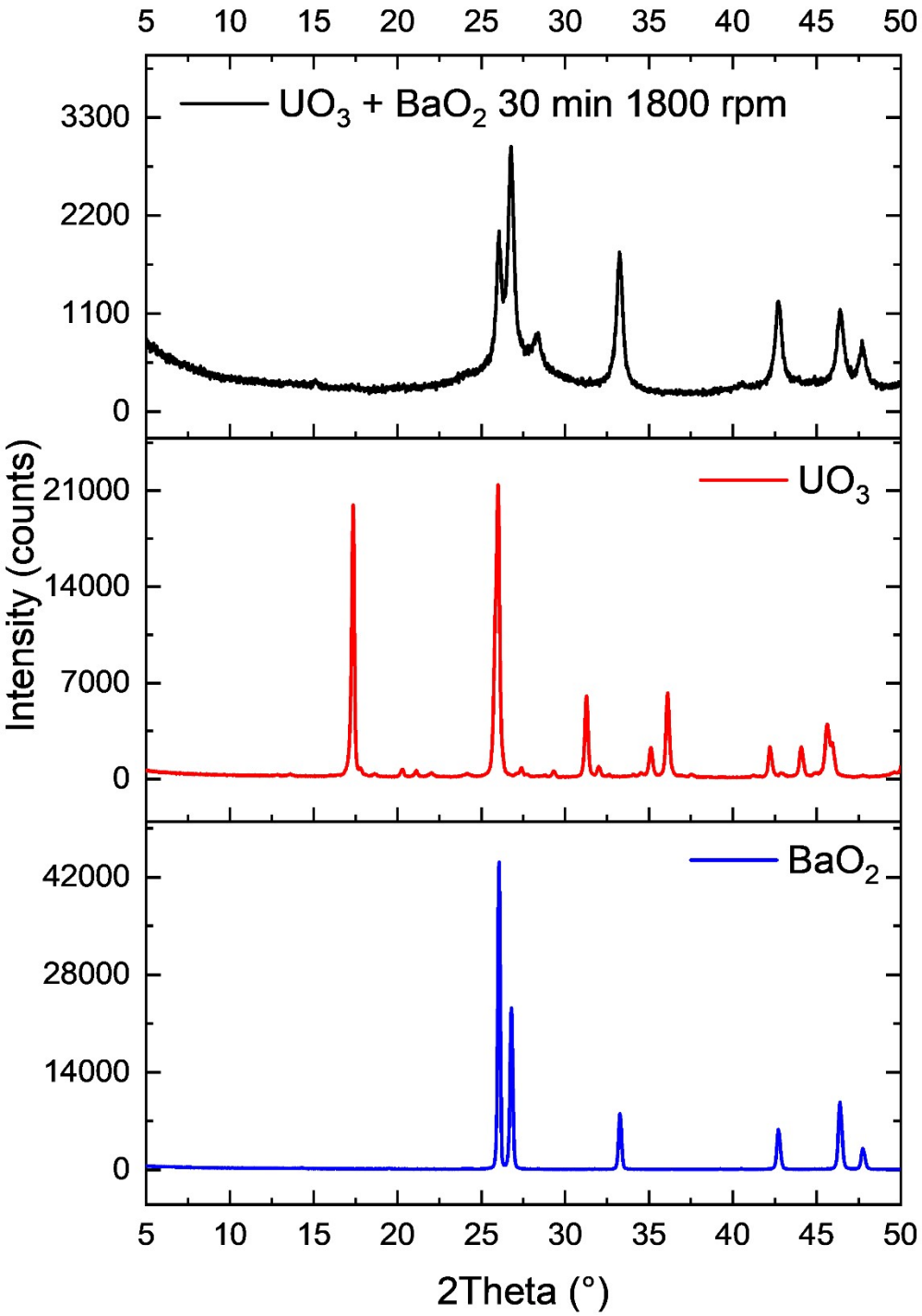

Figure S10: Raw PXRD patterns of UO_3 + BaO_2 30 min 1800 rpm and starting materials

Raman Spectroscopy

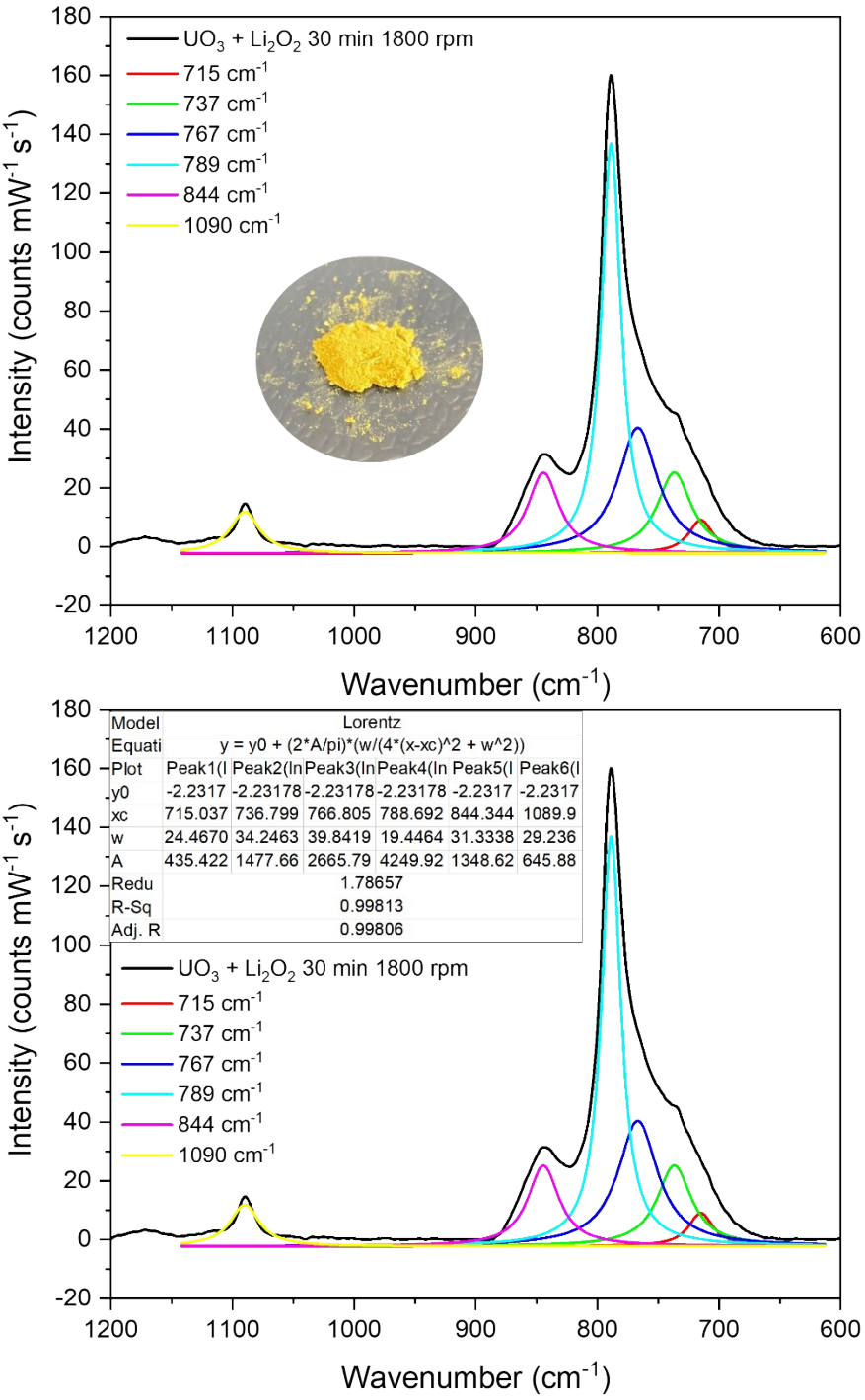

Figure S11: Raman fitting parameters of solid m_{30}-UO_3-Li_2O_2

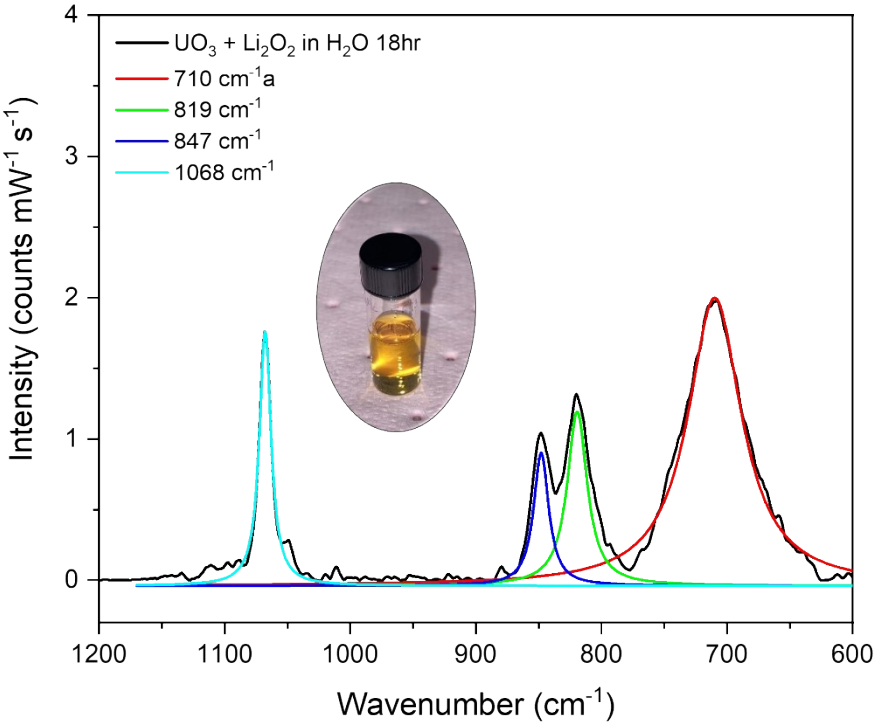

Model	Lorentz			
Equation	y = y0 + (2*A/pi)*(w/(4*(x-xc)^2 + w^2))			
Plot	Peak1(Intensity)	Peak2(Intensity)	Peak3(Intensity)	Peak4(Intensity)
y0	-0.04024 ± 0.00432	-0.04024 ± 0.00432	-0.04024 ± 0.00432	-0.04024 ± 0.00432
xc	709.7364 ± 0.1847	819.23929 ± 0.19917	847.92509 ± 0.22138	1067.63356 ± 0.09732
w	51.8105 ± 0.60593	19.19319 ± 0.65466	14.49081 ± 0.72552	11.3212 ± 0.29162
A	165.93533 ± 1.60263	37.18938 ± 1.03236	21.44418 ± 0.88775	32.01175 ± 0.61759
Reduced Chi-Sqr	0.00426			
R-Square (COD)	0.9847			
Adj. R-Square	0.98438			

UO3 + Li2O2 in H2O 18hr
710 cm-1a
819 cm-1
847 cm-1
1068 cm-1
Intensity (counts mW-1 s-1)
Wavenumber (cm-1)
4
3
2
1
0
1200
1100
1000
900
800
700
600

Figure S12: Raman fitting parameters of dissolved m_{30}-UO_3-Li_2O_2 in H_2O 18 hr

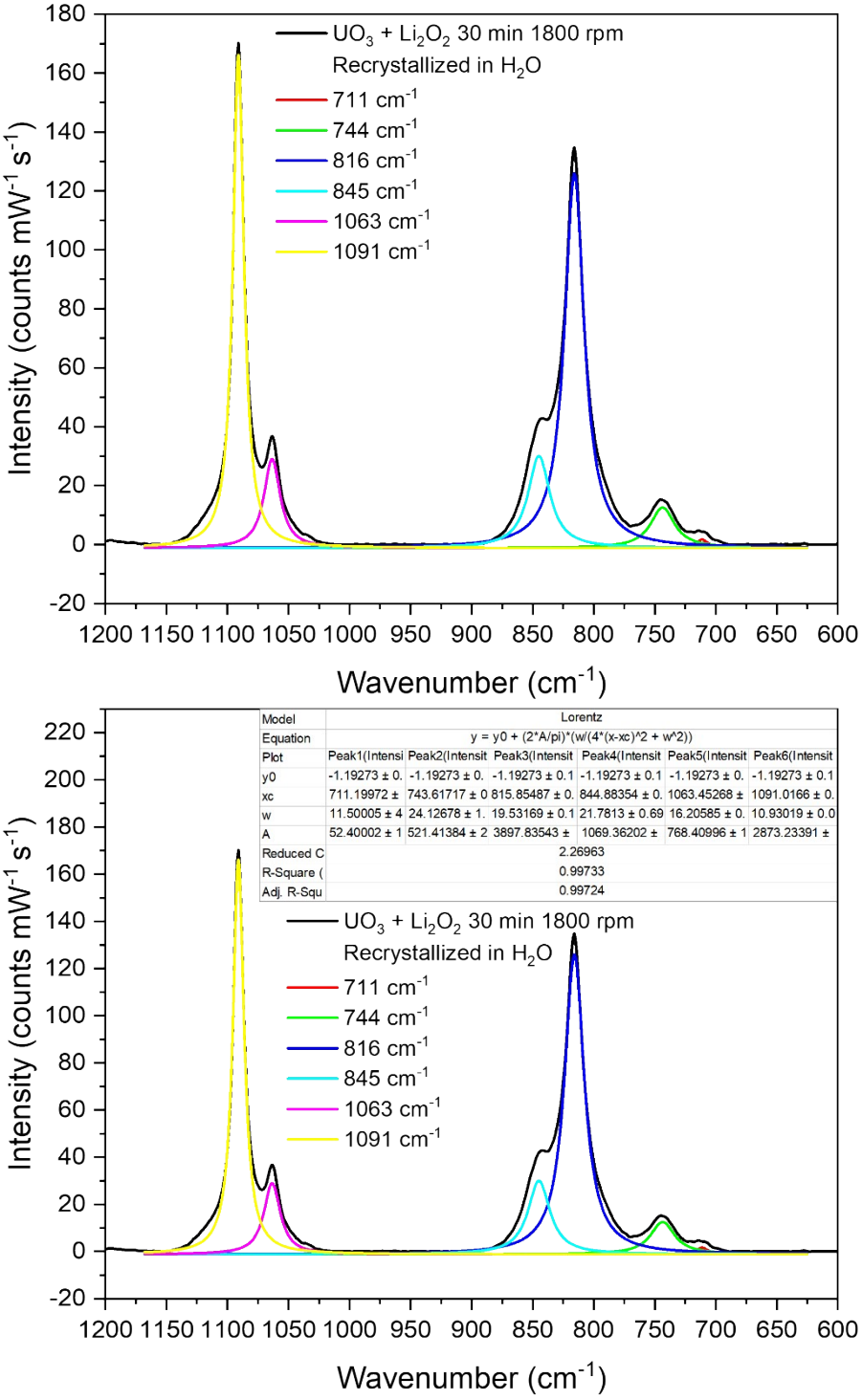

Figure S13: Raman fitting parameters of recrystallized m_{30}-UO_3-Li_2O_2

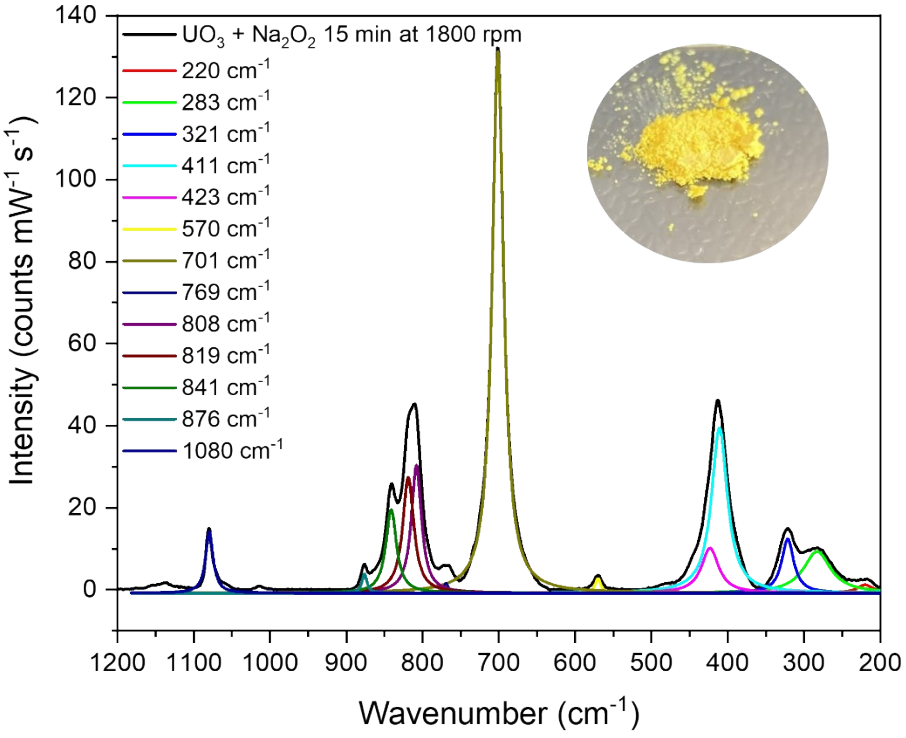

Model	Lorentz												
Equati	y = y0 + (2*A/pi)*(w/(4*(x-xc)^2 + w^2))												
Plot	Peak1(I	Peak2(I	Peak3(I	Peak4(In	Peak5(I	Peak6(I	Peak7(I	Peak8(I	Peak9(I	Peak10(	Peak11	Peak12	Peak13(
y0	-0.8123	-0.8123	-0.8123	-0.8123	-0.8123	-0.8123	-0.8123	-0.8123	-0.8123	-0.8123	-0.8123	-0.8123	-0.8123
xc	220.17	282.996	321.475	410.919	423.255	570.19	701.277	769.31	808.126	818.767	841.21	876.23	1079.54
w	24.850	43.1996	19.2877	25.0319	27.2798	8.4099	18.0789	6.9973	16.0045	17.5675	16.802	7.8756	11.9305
A	79.015	685.627	400.111	1582.55	469.500	46.647	3748.10	26.285	784.901	779.624	536.95	57.704	279.681
Redu	0.90518												
R-Squ	0.99703												
Adj. R	0.99691												

UO3 + Na2O2 15 min at 1800 rpm
220 cm-1
283 cm-1
321 cm-1
411 cm-1
423 cm-1
570 cm-1
701 cm-1
769 cm-1
808 cm-1
819 cm-1
841 cm-1
876 cm-1
1080 cm-1
Intensity (counts mW-1 s-1)
Wavenumber (cm-1)

Figure S14: Raman fitting parameters of solid m_{15}-UO_3-Na_2O_2

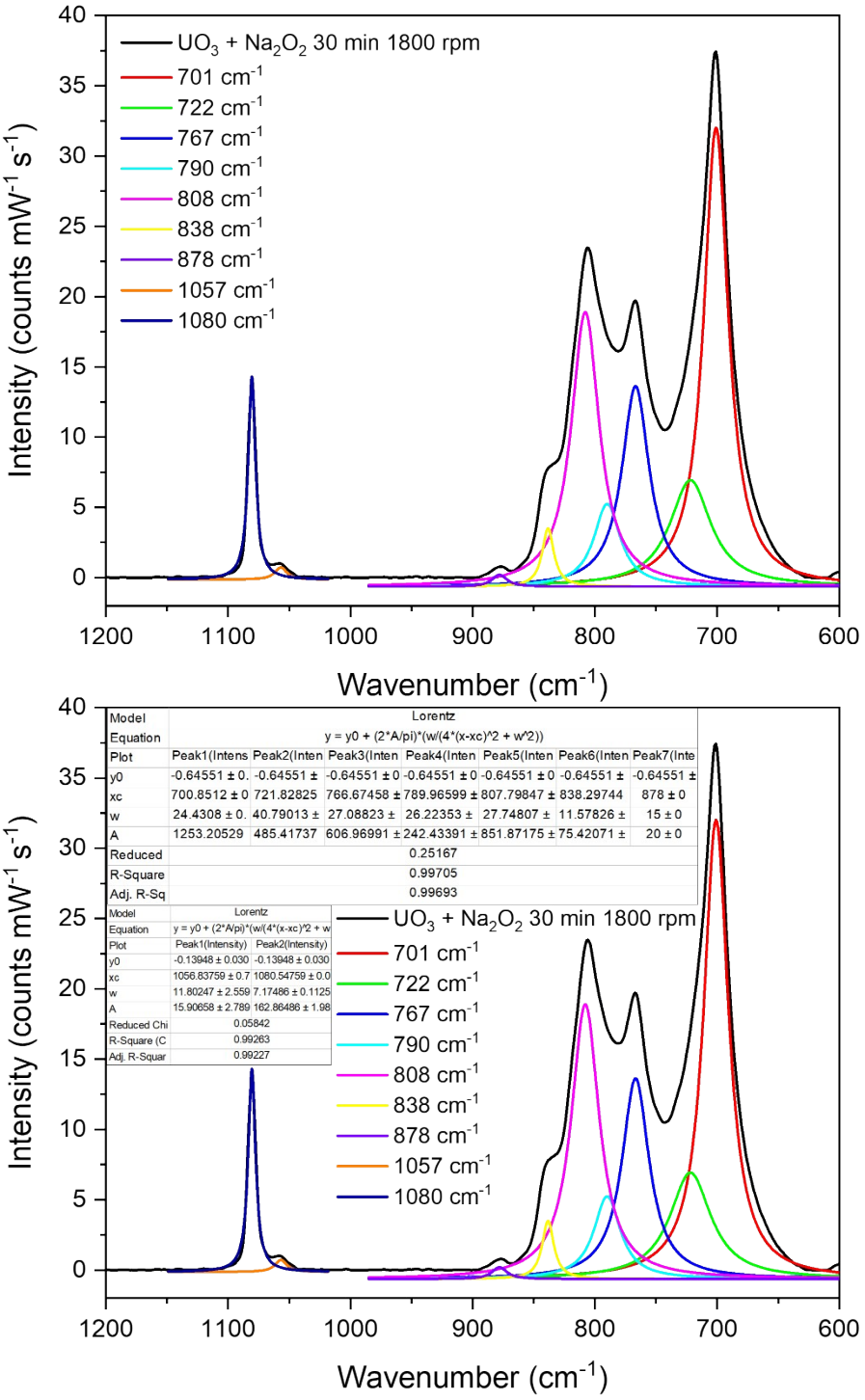

Figure S17: Raman fitting parameters of recrystallized m_{30}-UO_3-Na_2O_2

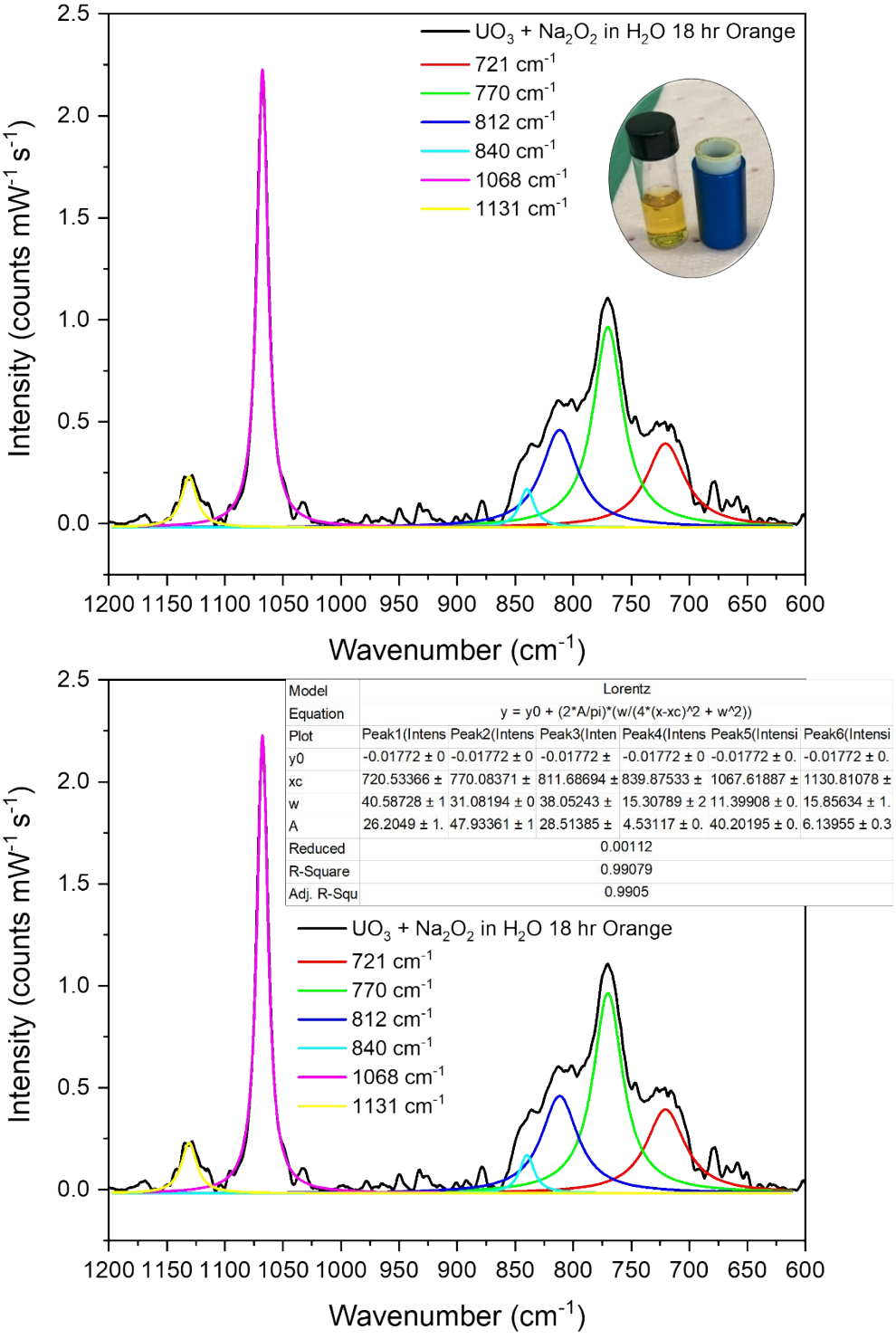

Model	Lorentz					
Equation	y = y0 + (2*A/pi)*(w/(4*(x-xc)^2 + w^2))					
Plot	Peak1(Intens	Peak2(Intens	Peak3(Inten	Peak4(Intens	Peak5(Intensi	Peak6(Intensi
y0	-0.01772 ± 0	-0.01772 ± 0	-0.01772 ±	-0.01772 ± 0	-0.01772 ± 0.	-0.01772 ± 0.
xc	720.53366 ±	770.08371 ±	811.68694 ±	839.87533 ±	1067.61887 ±	1130.81078 ±
w	40.58728 ± 1	31.08194 ± 0	38.05243 ±	15.30789 ± 2	11.39908 ± 0.	15.85634 ± 1.
A	26.2049 ± 1.	47.93361 ± 1	28.51385 ±	4.53117 ± 0.	40.20195 ± 0.	6.13955 ± 0.3
Reduced	0.00112					
R-Square	0.99079					
Adj. R-Squ	0.9905					

Figure S16: Raman fitting parameters of dissolved m_{30}-UO_3-Na_2O_2 in H_2O 18 hr

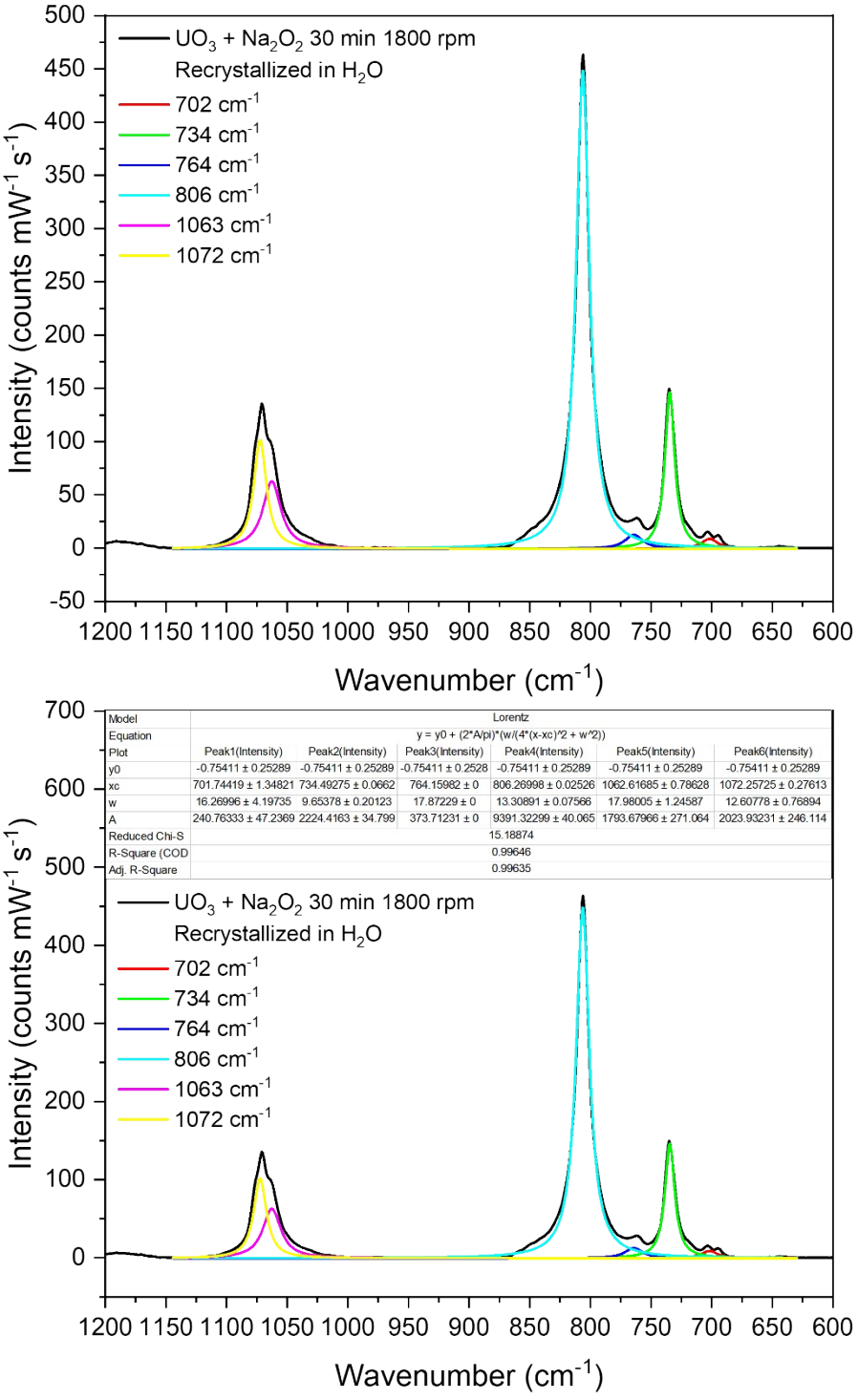

Model	Lorentz					
Equation	y = y0 + (2*A/pi)*(w/(4*(x-xc)^2 + w^2))					
Plot	Peak1(Intensity)	Peak2(Intensity)	Peak3(Intensity)	Peak4(Intensity)	Peak5(Intensity)	Peak6(Intensity)
y0	-0.75411 ± 0.25289	-0.75411 ± 0.25289	-0.75411 ± 0.2528	-0.75411 ± 0.25289	-0.75411 ± 0.25289	-0.75411 ± 0.25289
xc	701.74419 ± 1.34821	734.49275 ± 0.0662	764.15982 ± 0	806.26998 ± 0.02526	1062.61685 ± 0.78628	1072.25725 ± 0.27613
w	16.26996 ± 4.19735	9.65378 ± 0.20123	17.87229 ± 0	13.30891 ± 0.07566	17.98005 ± 1.24587	12.60778 ± 0.76894
A	240.76333 ± 47.2369	2224.4163 ± 34.799	373.71231 ± 0	9391.32299 ± 40.065	1793.67966 ± 271.064	2023.93231 ± 246.114
Reduced Chi-S	15.18874					
R-Square (COD	0.99646					
Adj. R-Square	0.99635					

Figure S17: Raman fitting parameters of recrystallized m_{30}-UO_3-Na_2O_2

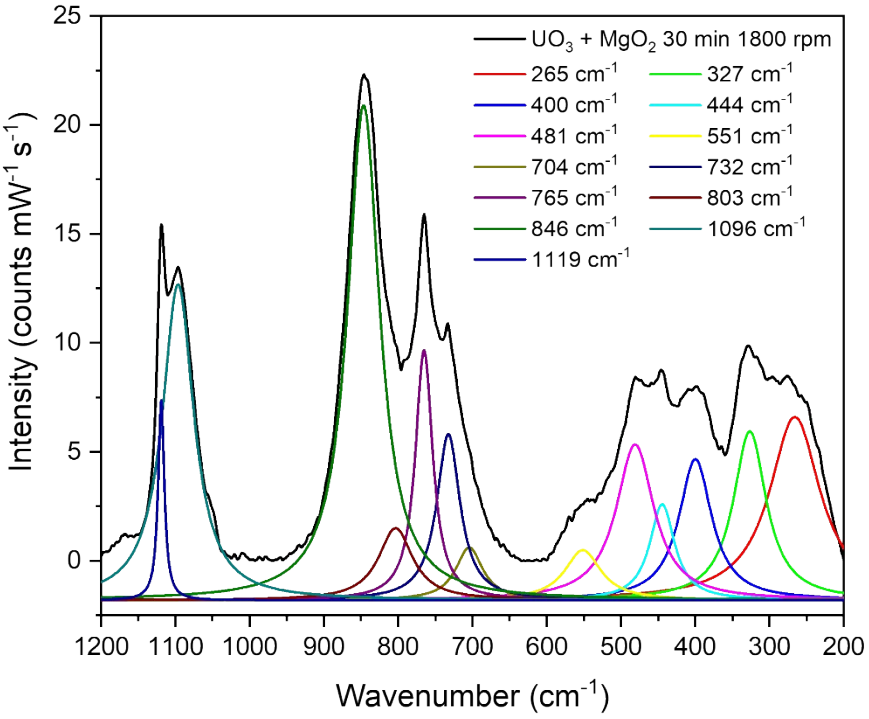

Mod	Lorentz											
Equ	y = y0 + (2*A/pi)*(w/(4*(x-xc)^2 + w^2))											
Plot	Peak1	Peak2	Peak	Peak4	Peak5	Peak6	Peak7	Peak8	Peak9	Peak1	Peak1	Peak1	Peak1
y0	-1.810	-1.810	-1.81	-1.810	-1.810	-1.810	-1.810	-1.810	-1.810	-1.810	-1.810	-1.810	-1.810
xc	265.9	326.5	399.8	444.5	481.0	551.3	704.3	732.4	765.2	803.5	846.5	1096.	1119.
w	83.20	53.88	53.77	40.71	61.90	59.26	44.01	38.03	28.25	55.99	52.48	51.23	9.991
A	1099.	656.2	547.0	281.7	695.1	214.3	167.8	455.1	509.5	291.1	1872.	1166.	143.8
Red	0.12707												
R-S	0.99522												
Adj.	0.99503												

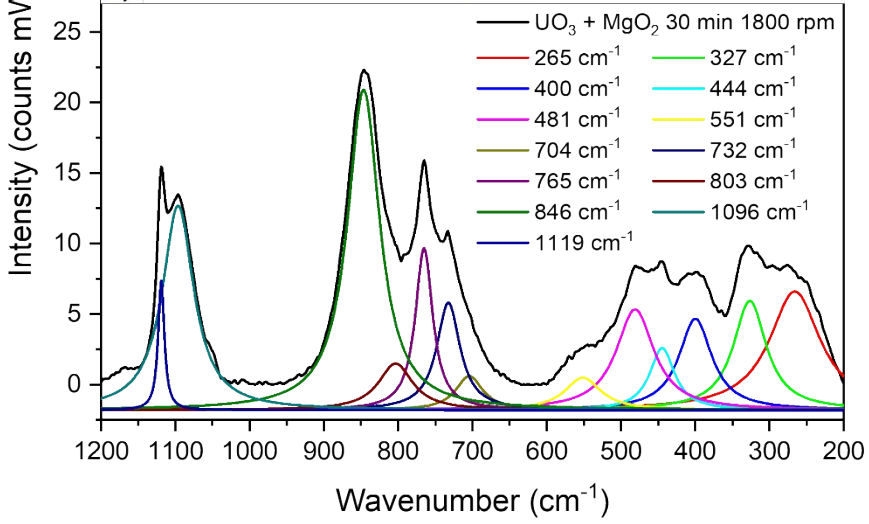

Figure S18: Raman fitting parameters of solid UO_3 + MgO_2 30 min 1800 rpm

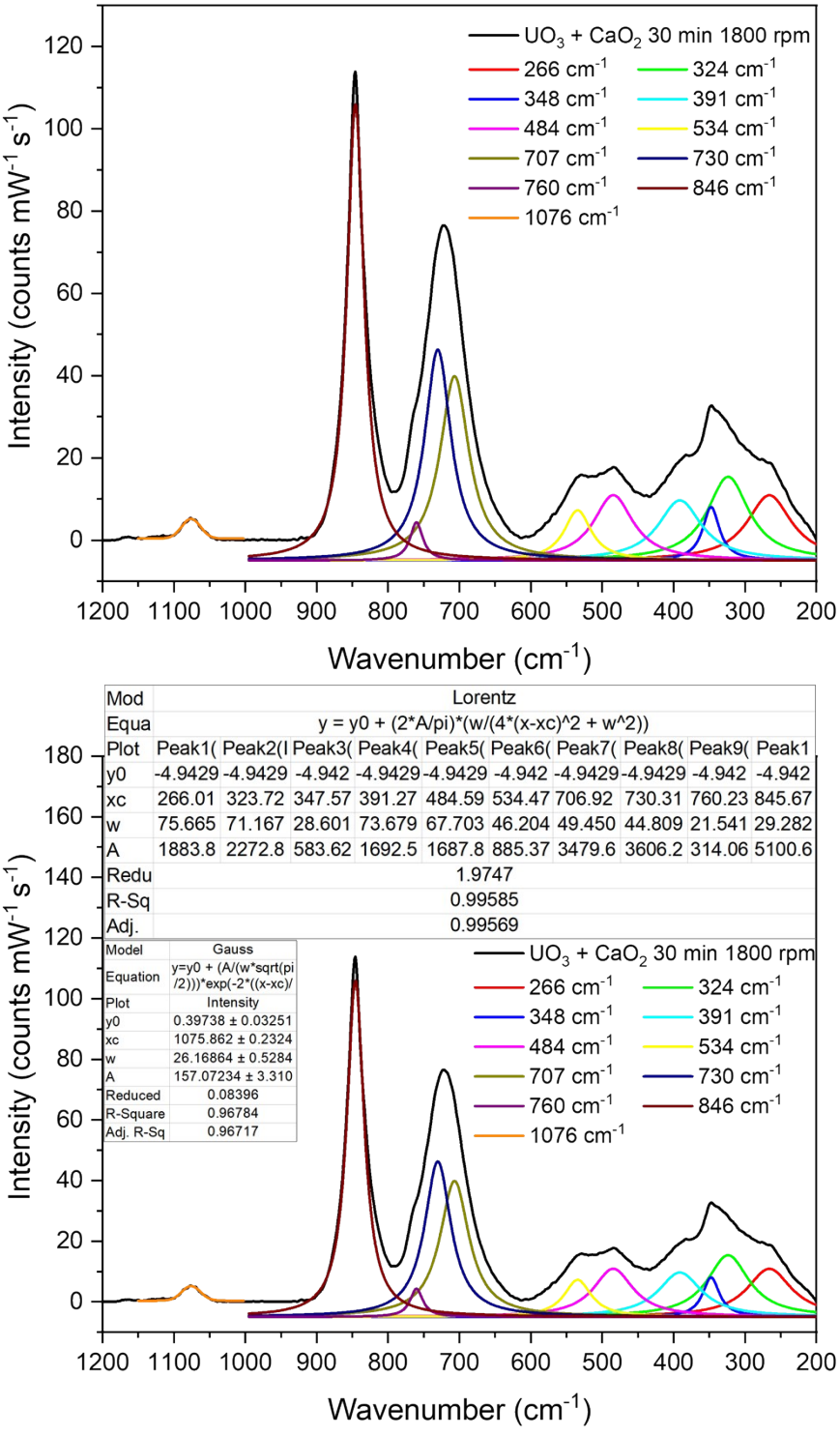

Figure S19: Raman fitting parameters of solid UO_3 + CaO_2 30 min 1800 rpm

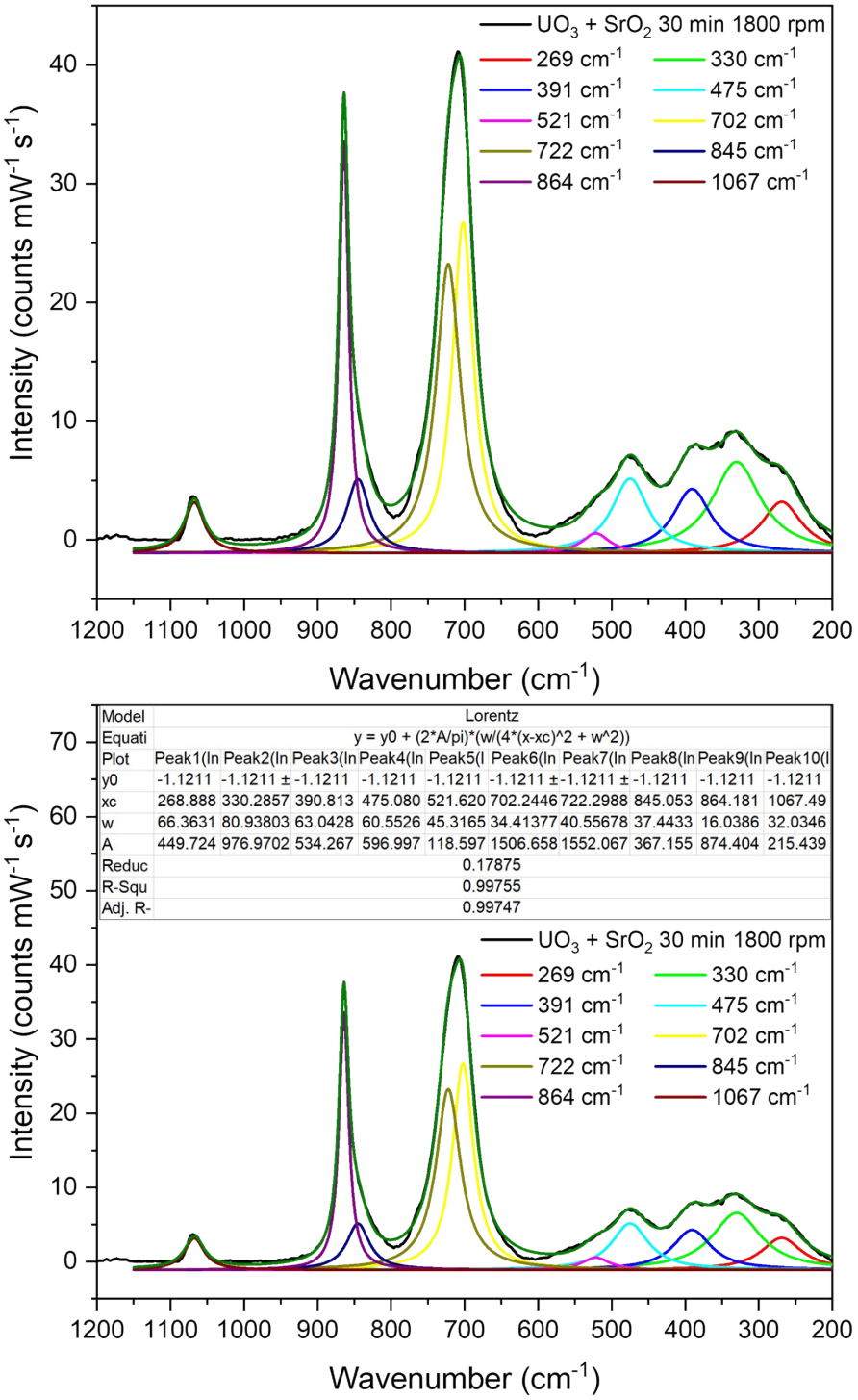

Model	Lorentz									
Equati	y = y0 + (2*A/pi)*(w/(4*(x-xc)^2 + w^2))									
Plot	Peak1(In	Peak2(In	Peak3(In	Peak4(In	Peak5(I	Peak6(In	Peak7(In	Peak8(In	Peak9(In	Peak10(I
y0	-1.1211	-1.1211 ±	-1.1211	-1.1211	-1.1211	-1.1211 ±	-1.1211 ±	-1.1211	-1.1211	-1.1211
xc	268.888	330.2857	390.813	475.080	521.620	702.2446	722.2988	845.053	864.181	1067.49
w	66.3631	80.93803	63.0428	60.5526	45.3165	34.41377	40.55678	37.4433	16.0386	32.0346
A	449.724	976.9702	534.267	596.997	118.597	1506.658	1552.067	367.155	874.404	215.439
Reduc	0.17875									
R-Squ	0.99755									
Adj. R-	0.99747									

Figure S20: Raman fitting parameters of solid UO_3 + SrO_2 30 min 1800 rpm

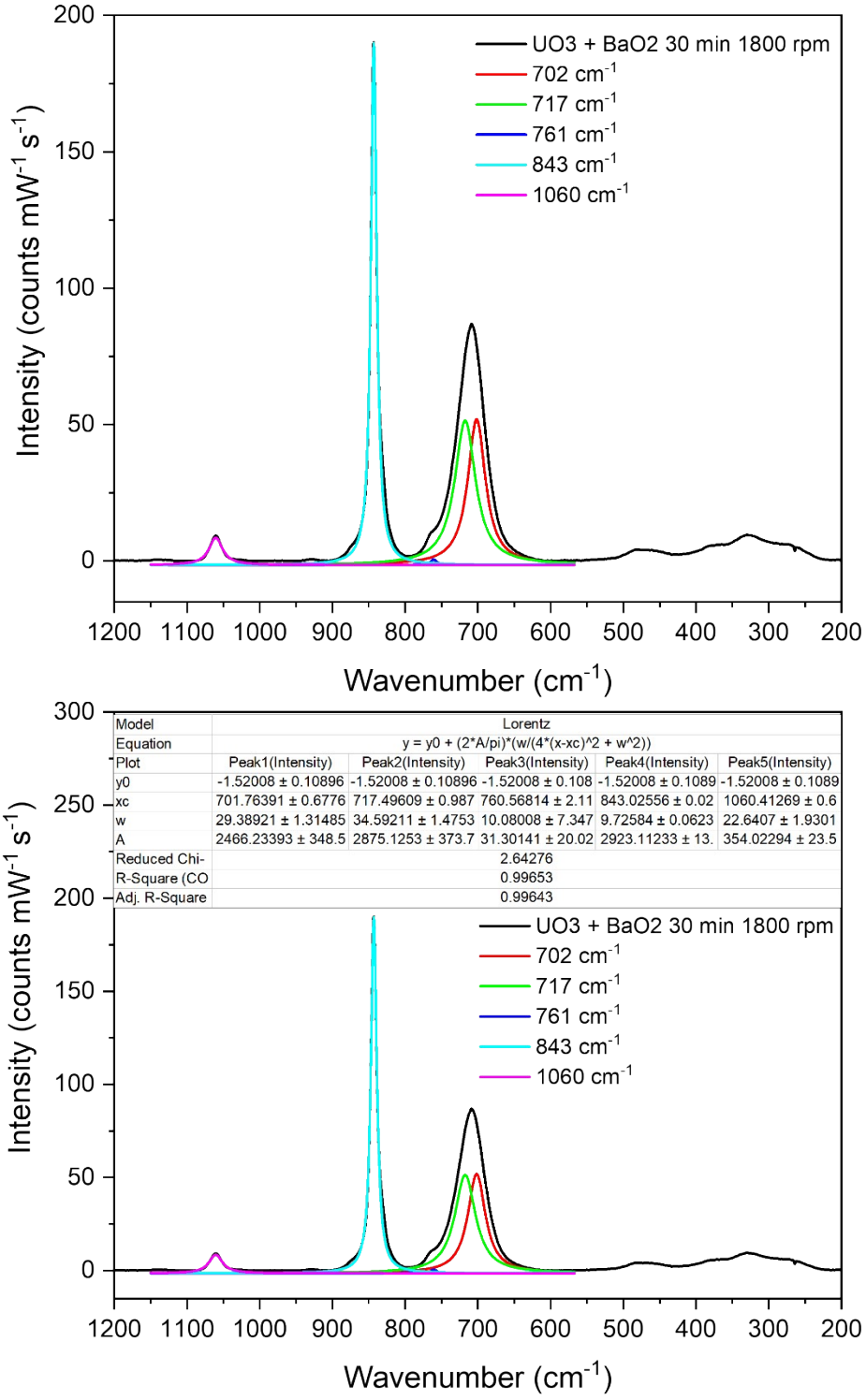

Model	Lorentz				
Equation	y = y0 + (2*A/pi)*(w/(4*(x-xc)^2 + w^2))				
Plot	Peak1(Intensity)	Peak2(Intensity)	Peak3(Intensity)	Peak4(Intensity)	Peak5(Intensity)
y0	-1.52008 ± 0.10896	-1.52008 ± 0.10896	-1.52008 ± 0.108	-1.52008 ± 0.1089	-1.52008 ± 0.1089
xc	701.76391 ± 0.6776	717.49609 ± 0.987	760.56814 ± 2.11	843.02556 ± 0.02	1060.41269 ± 0.6
w	29.38921 ± 1.31485	34.59211 ± 1.4753	10.08008 ± 7.347	9.72584 ± 0.0623	22.6407 ± 1.9301
A	2466.23393 ± 348.5	2875.1253 ± 373.7	31.30141 ± 20.02	2923.11233 ± 13.	354.02294 ± 23.5
Reduced Chi-	2.64276				
R-Square (CO	0.99653				
Adj. R-Square	0.99643				

UO3 + BaO2 30 min 1800 rpm
702 cm-1
717 cm-1
761 cm-1
843 cm-1
1060 cm-1
Intensity (counts mW-1 s-1)
Wavenumber (cm-1)
300
250
200
150
100
50
0
1200 1100 1000 900 800 700 600 500 400 300 200

Figure S21: Raman fitting parameters of solid UO_3 + BaO_2 30 min 1800 rpm

Infrared Spectroscopy

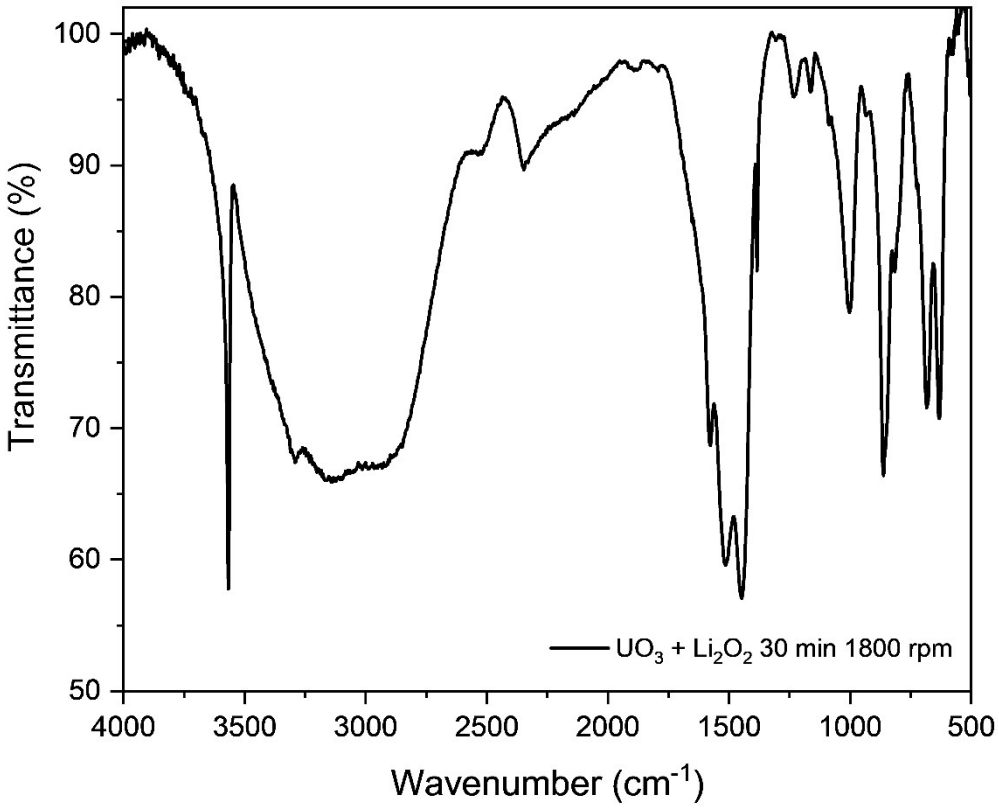

Figure S22: Infrared spectrum of solid m_{30}-UO_3-Li_2O_2

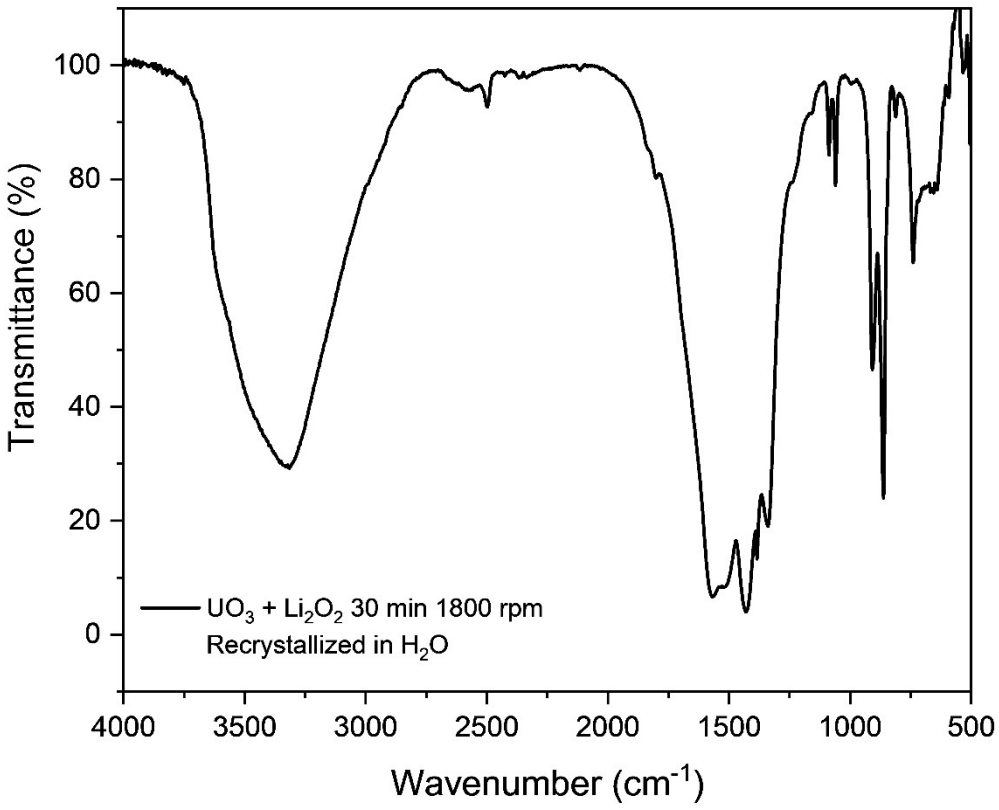

Figure S23: Infrared spectrum of recrystallized m_{30}-UO_3-Li_2O_2

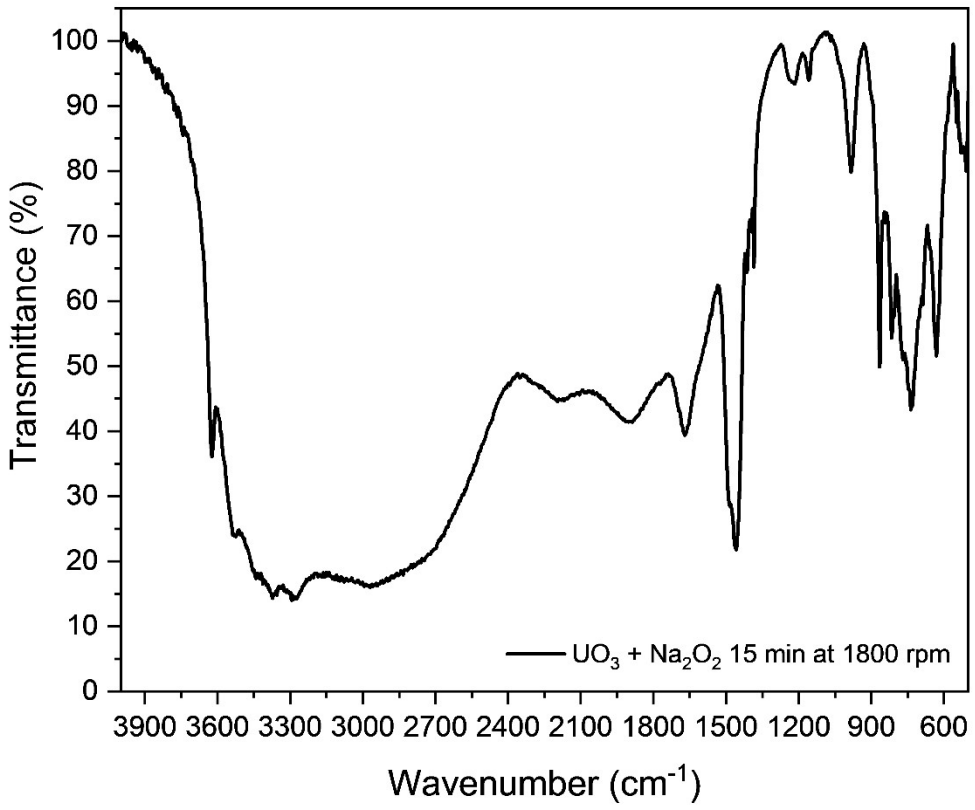

Figure S24: Infrared spectrum of solid m_{15}-UO_3-Na_2O_2

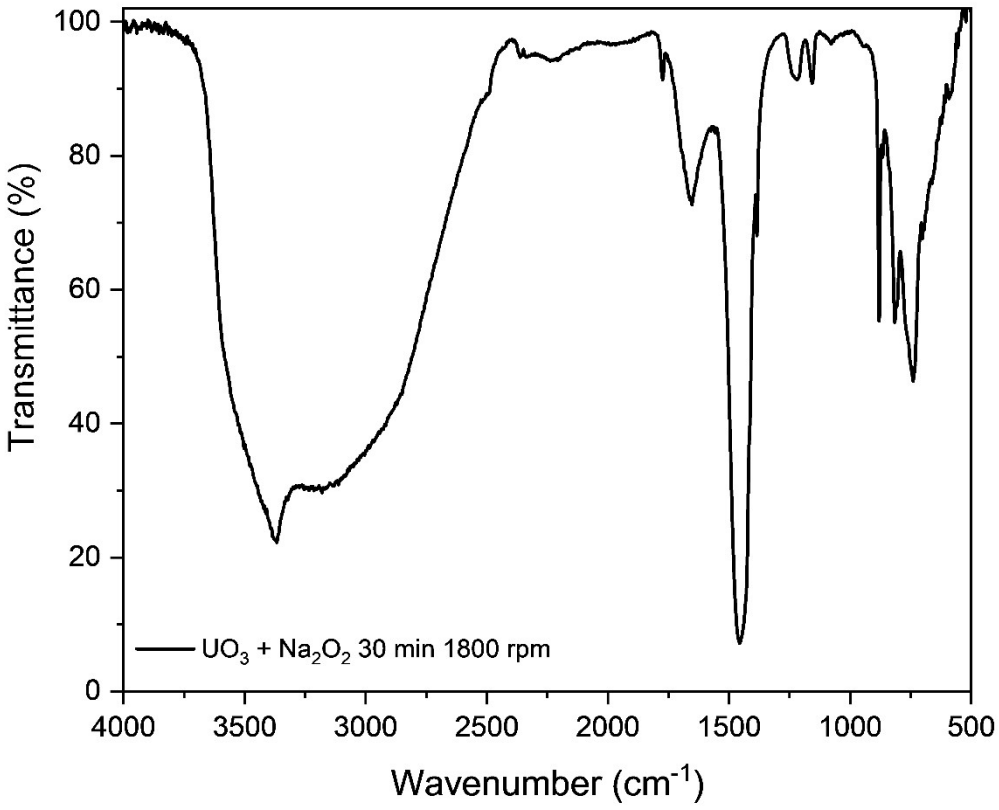

Figure S25: Infrared spectrum of solid m_{30}-UO_3-Na_2O_2

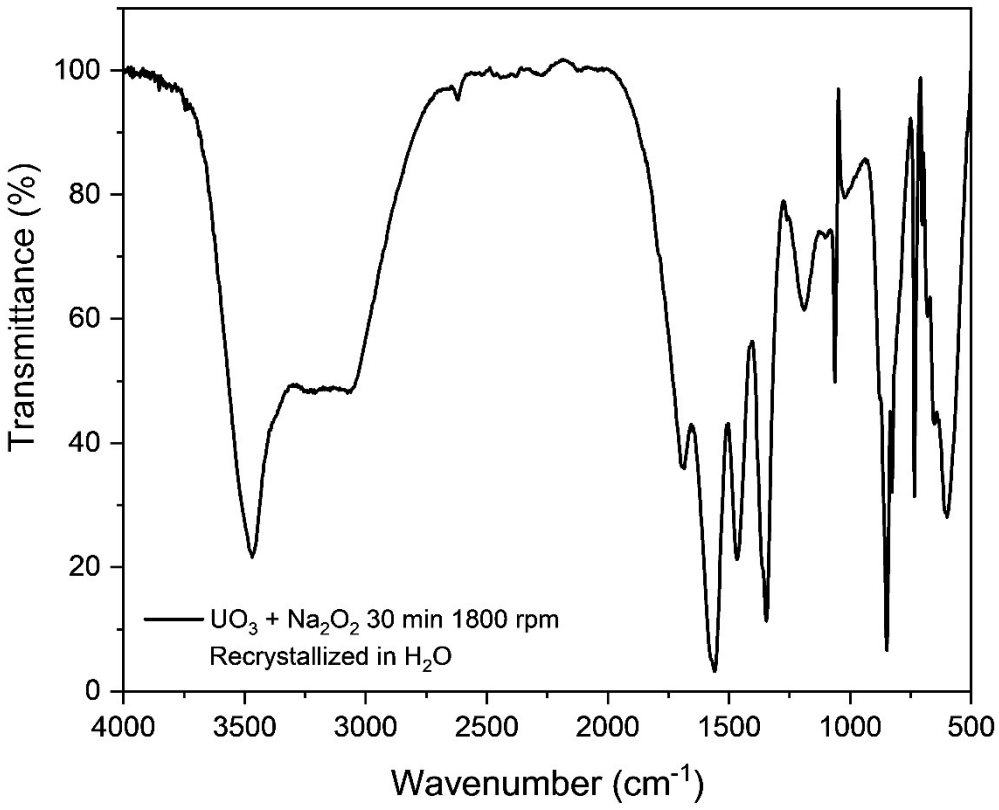

Figure S26: Infrared spectrum of recrystallized m_{30}-UO_3-Na_2O_2

Scanning Electron Microscopy

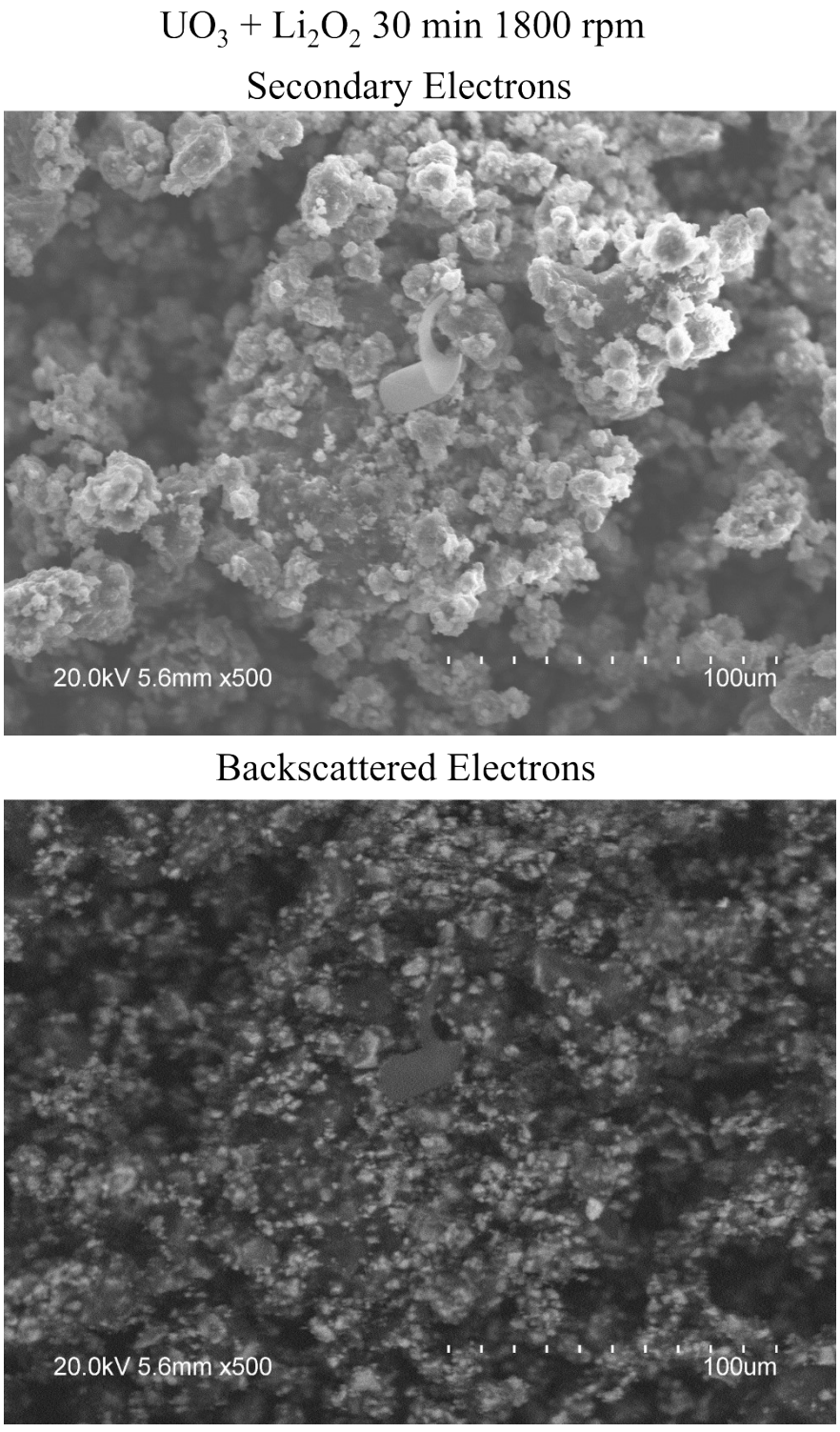

Figure S29: Secondary and backscattered images of recrystallized m_{30}-UO_3-Li_2O_2

$UO_3 + Li_2O_2$ 30 min 1800 rpm

Secondary Electrons

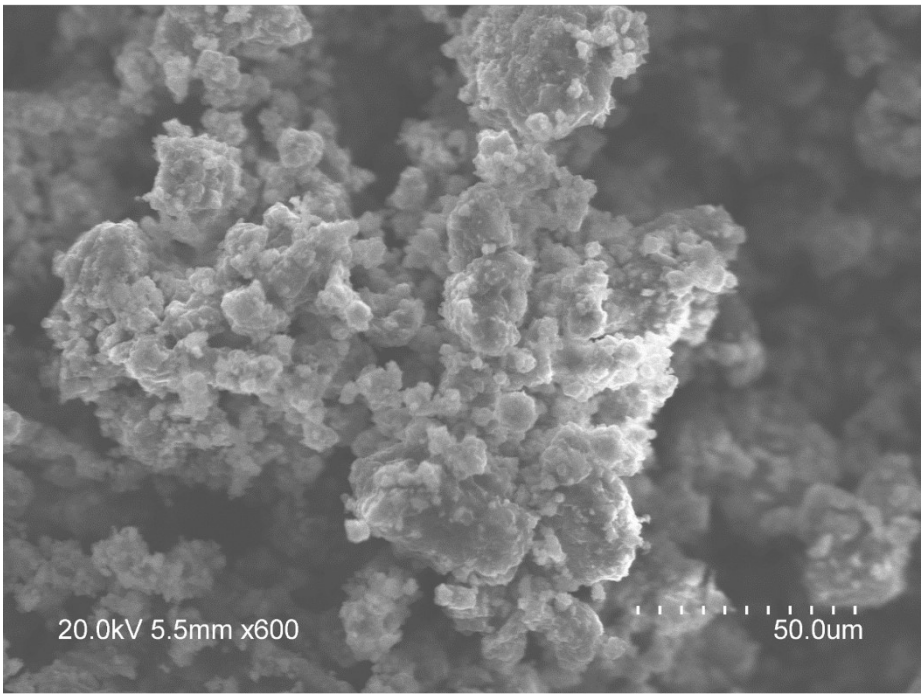

Backscattered Electrons

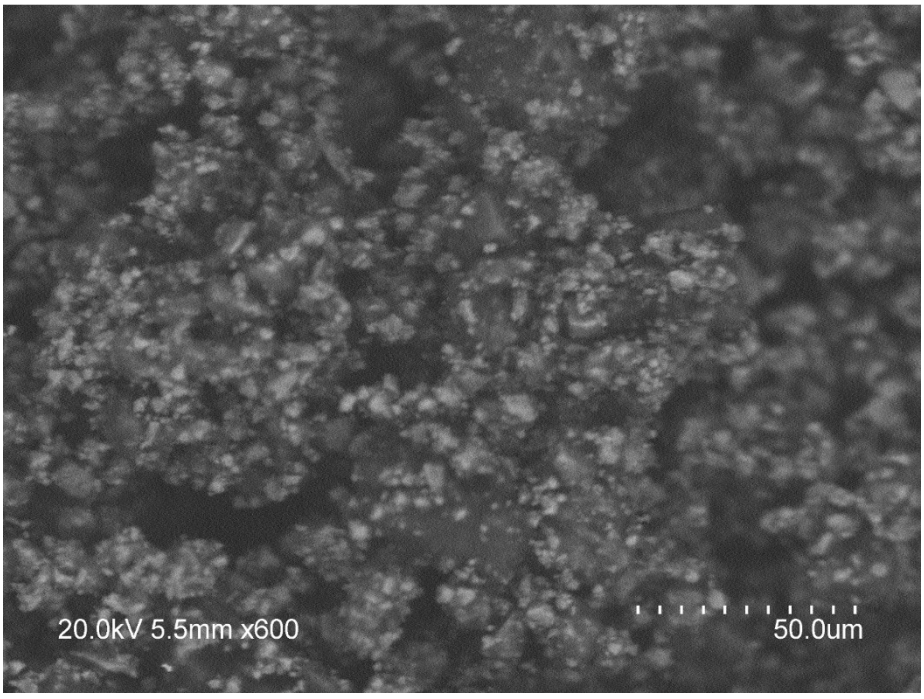

Figure S28: Secondary and backscattered images of solid m_{30}-UO_3-Li_2O_2

UO_3 + Li_2O_2 30 min 1800 rpm H_2O recrystallized

Secondary Electrons

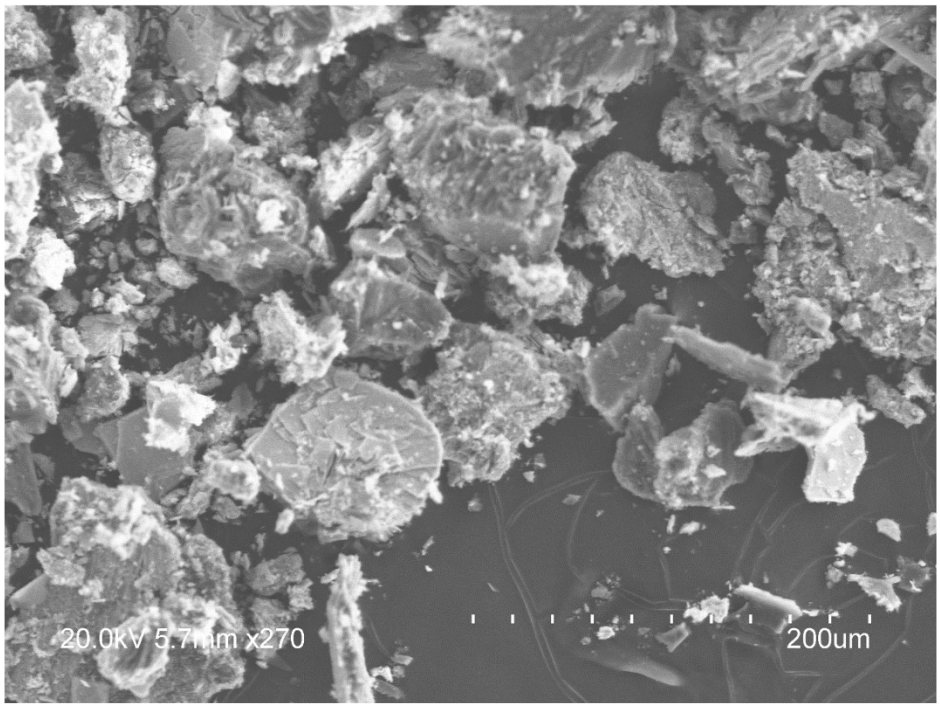

Backscattered Electrons

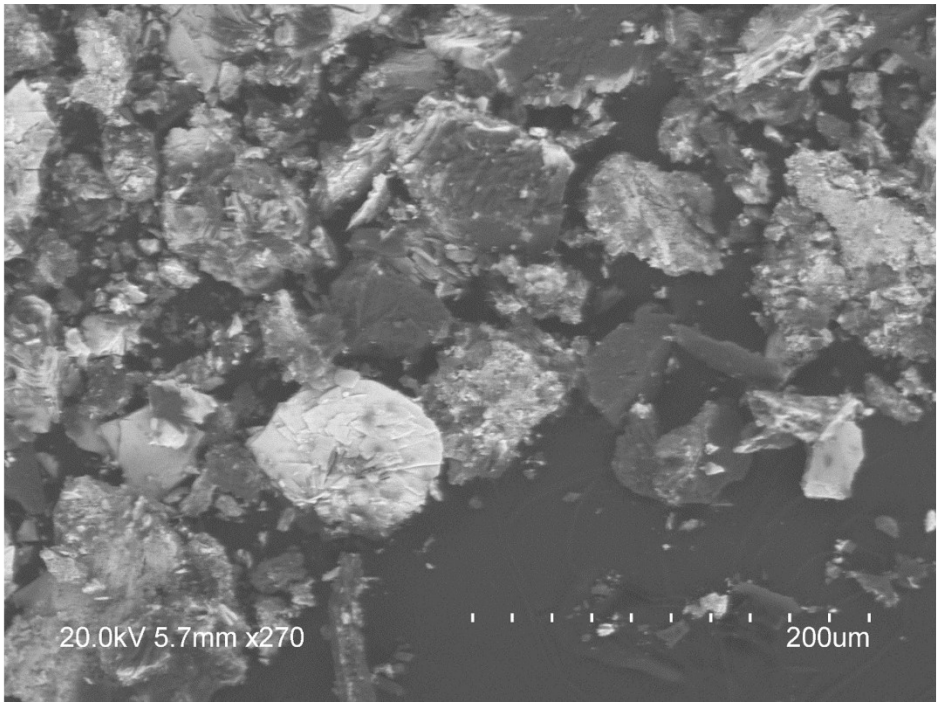

Figure S29: Secondary and backscattered images of recrystallized m_{30}-UO_3-Li_2O_2

UO_3 + Li_2O_2 30 min 1800 rpm H_2O recrystallized
Secondary Electrons

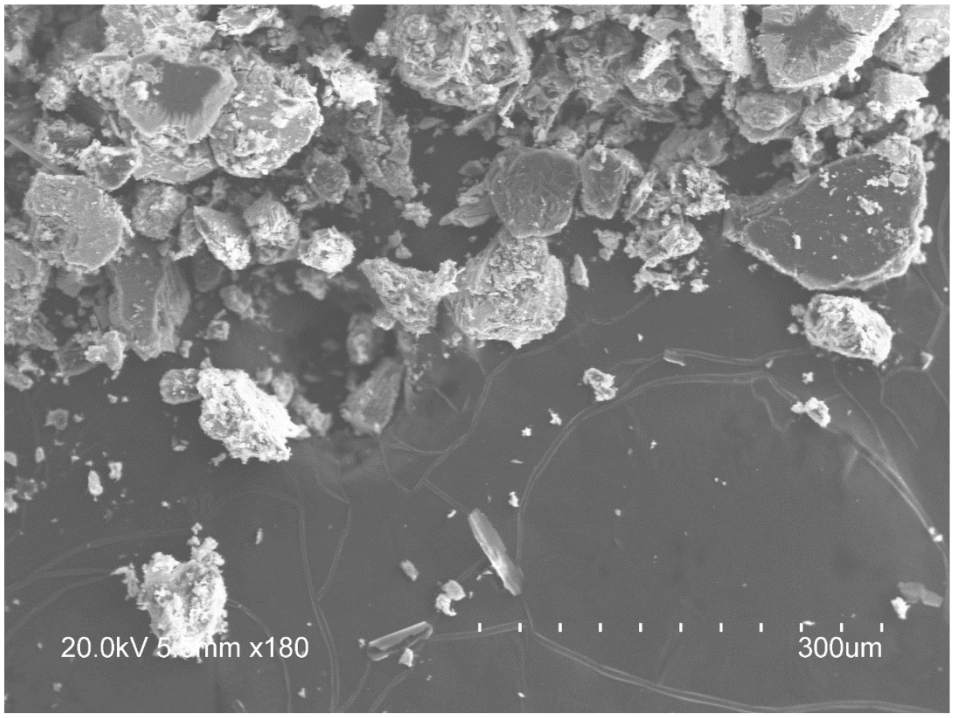

Backscattered Electrons

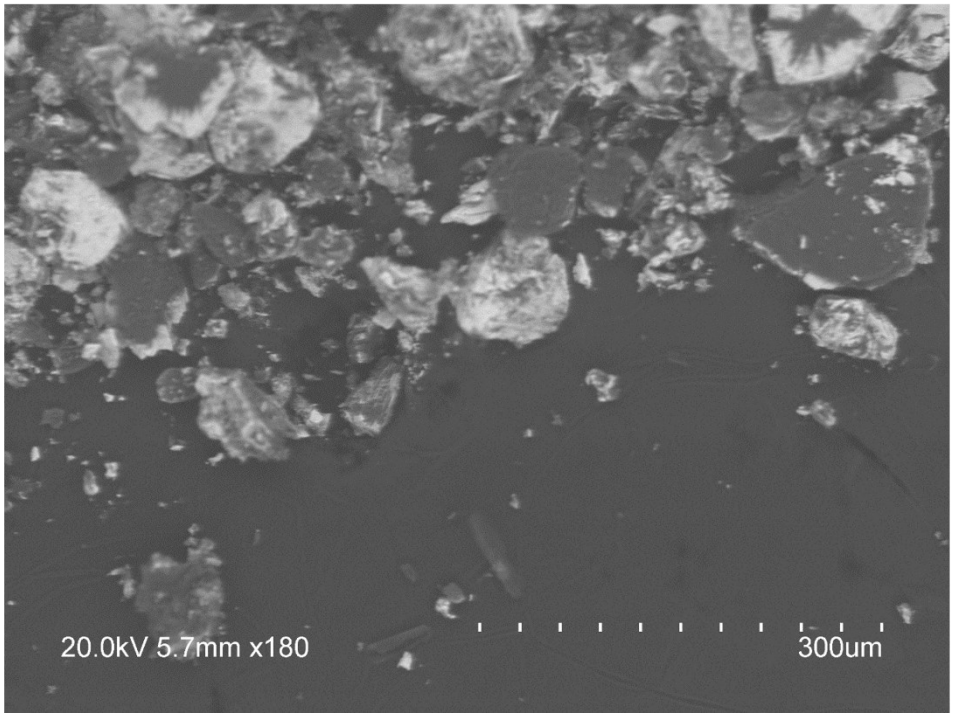

Figure S30: Secondary and backscattered images of recrystallized m_{30}-UO_3-Li_2O_2

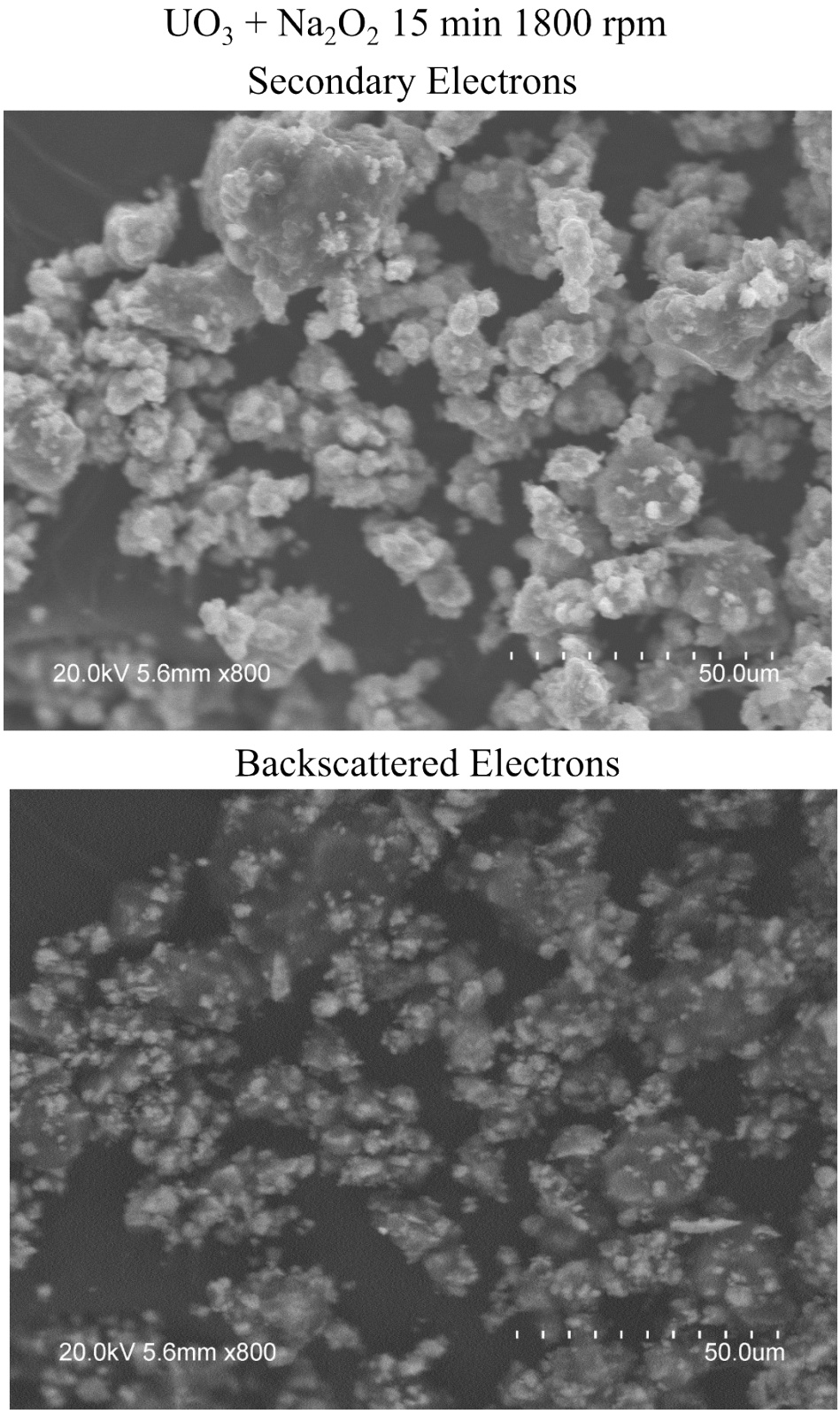

Figure S31: Secondary and backscattered images of solid m_{15}-UO_3-Na_2O_2

$UO_3 + Na_2O_2$ 30 min 1800 rpm

Secondary Electrons

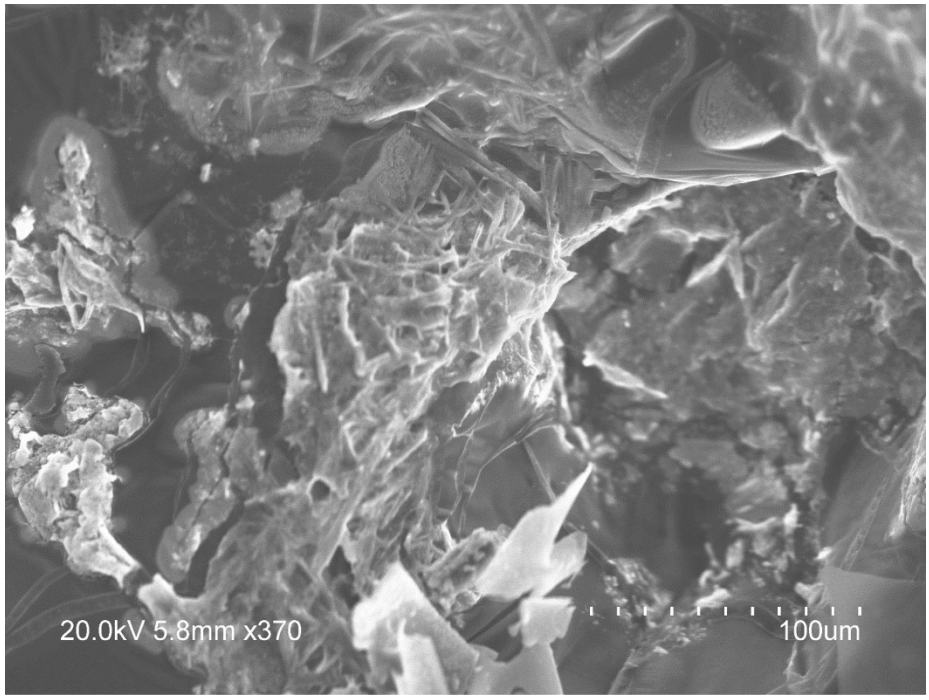

Backscattered Electrons

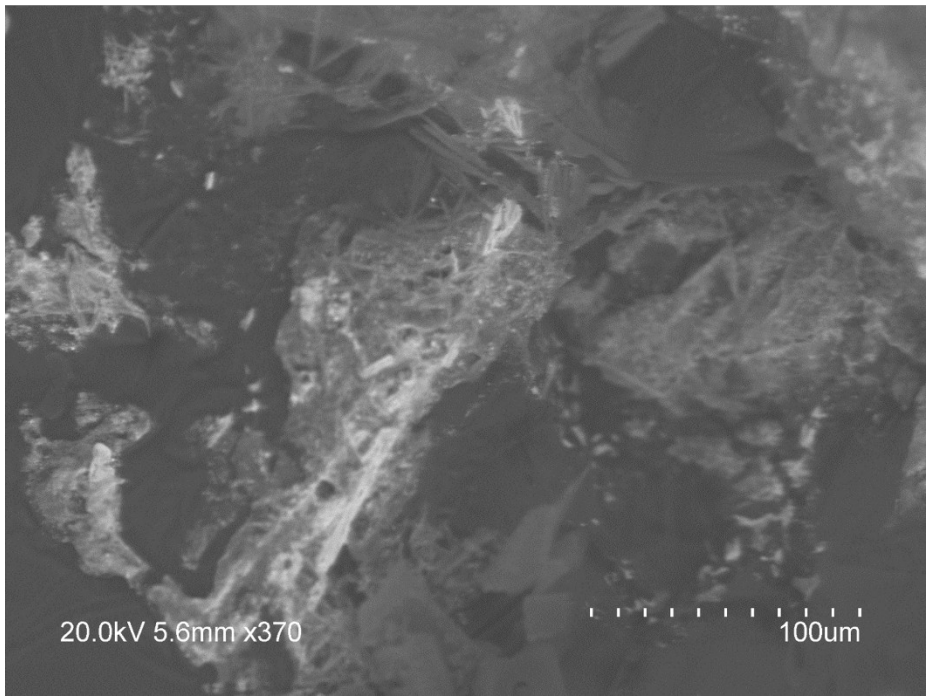

Figure S32: Secondary and backscattered images of solid m_{30}-UO_3-Na_2O_2

UO_3 + Na_2O_2 30 min 1800 rpm H_2O recrystallized

Secondary Electrons

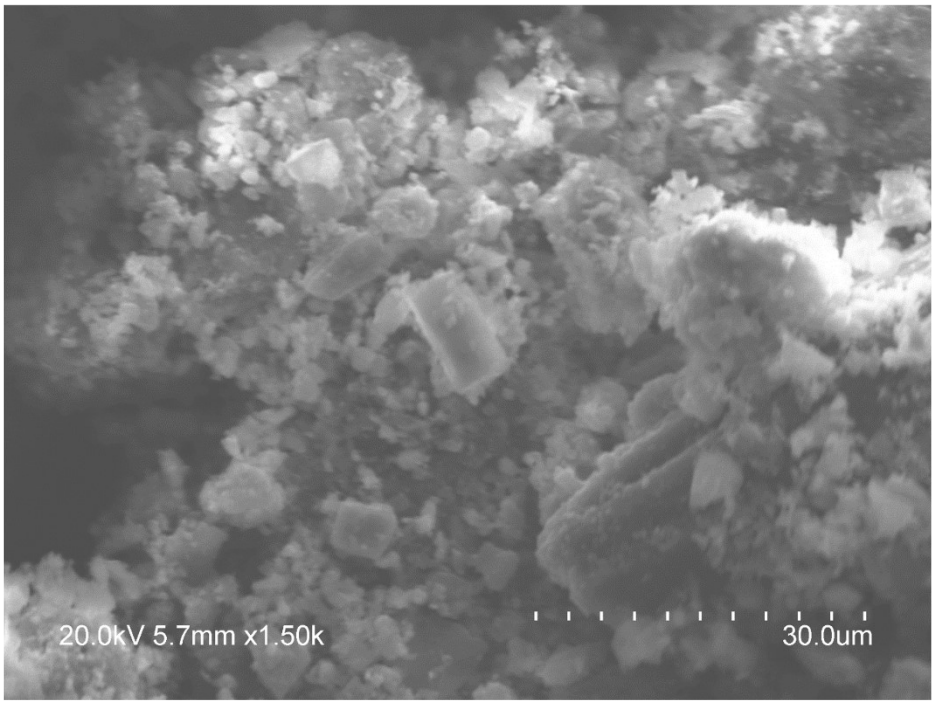

Backscattered Electrons

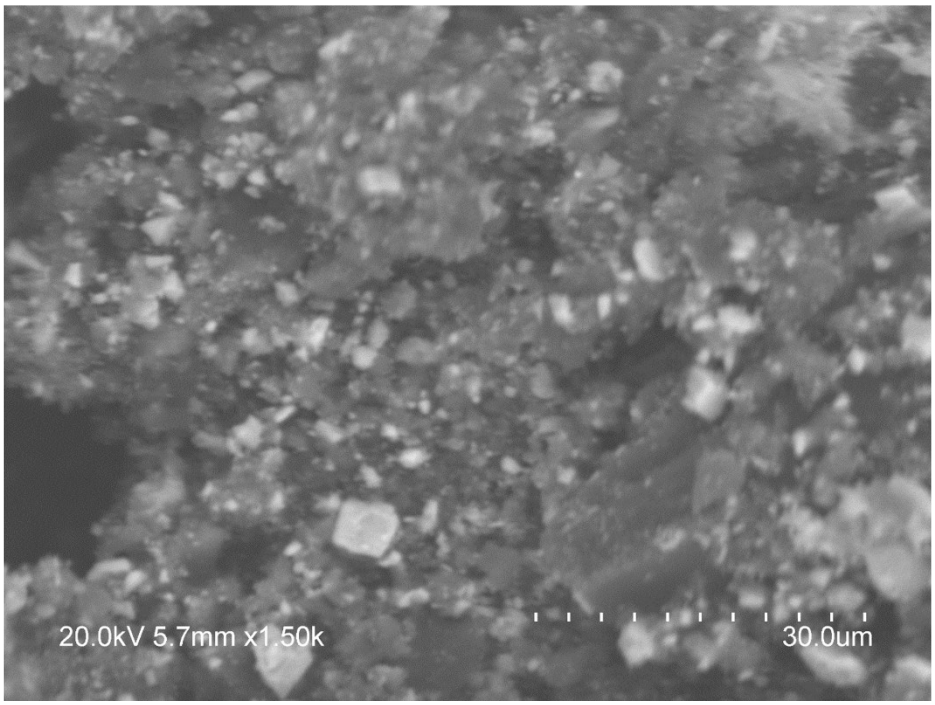

Figure S33: Secondary and backscattered images of recrystallized m_{30}-UO_3-Na_2O_2

Mechanism of Carbonate Formation

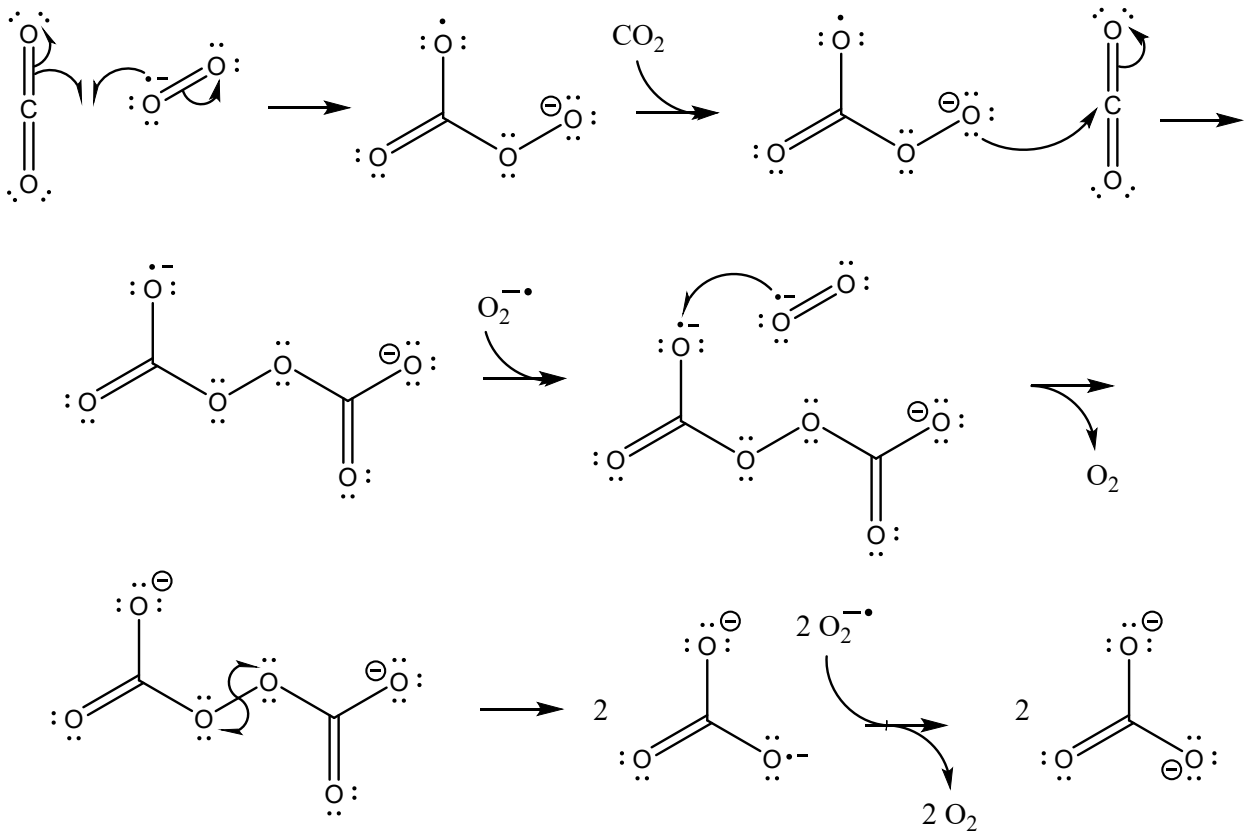

Figure S34: Mechanism of carbonate formation via mechanochemically induced superoxide anion interactions with molecular carbon dioxide.

Superoxide radicals $O_2^{\bullet -}$ are formed in the solid state due to mechanochemical impact on the solid starting materials Li_2O_2 and Na_2O_2 during grinding. The $O_2^{\bullet -}$ within the solid react with molecular CO_2 in gas form by inducing a homolytic cleavage of the C=O bond of the CO_2 carbonyl, which resulting in the formation of the C-O-O $^-$ peroxycarbonate adduct and a C-O$^{\bullet -}$ radical in place of carbonyl. The peroxycarbonate adduct C-O-**O** $^-$ performs a nucleophilic attack on the electrophilic carbon of another incoming CO_2 molecule, resulting in peroxydicarbonate anionic radical $C_2O_6^{\bullet -}$, which in turn accepts the unpaired electron from the superoxide radical $O_2^{\bullet -}$ resuling in the release of oxygen gas and formation of peroxydicarbonate anion. The peroxydicarbonate anion further undergoes a homolytic cleavage of the O-O bond yielding two equivalents of $CO_3^{\bullet -}$ species. Two $CO_3^{\bullet -}$ molecules stoichimetrically react with two superoxide radicals $O_2^{\bullet -}$ resulting in two equivalents of oxygen gas and two equivalents of carbonate anions CO_3^{2-}.